People's Democratic Republic of Algeria
Ministry of Higher Education and Scientific Research

University M'Hamed BOUGARA – Boumerdes

Institute of Electrical and Electronic Engineering

Department of Electronics

Final Year Project Report Presented in Partial Fulfilment of the Requirements for the Degree of

MASTER

In **Telecommunication**

Option: **Telecommunications**

Title:

Design of 4 Elements Linear Microstrip Antenna Array with Reduced Mutual Coupling and a Feeding Network

Presented by:

- **OUKIL Amira**
- **TOUAHRI Imane**

Supervisor:

Pr. A. AZRAR

Registration Number:……/2020

Dedication

The First special dedication goes to my parents, to my father, who I wished was here to see his little girl graduating and be proud of her. Although he is not here but he always pushed me to work hard, and believe in myself. To my mum, that I can never thank enough for being the mother and the father I can always count on. Her strengths and support, my constant source of inspiration, are beyond the imagination.

I would also like to dedicate this dissertation to my sisters and my brother. Naila, for her constant care and valuable advice when pushing me toward the good opportunities. Soumeya, for her mindful thoughts for the whole family and her ability to forgive anything. Amine, my only brother, for making me smile and forget the bad memories all the time. Hadjer, for always making me see the world differently, to have big dreams and always believing in it. The one that always wants me to succeed and see me growing all the time. To my little nephew, ANES, for being my source of happiness; and finally, to every member of my family who has been there for me.

Without forgetting my second family, my dearest best friends, my safe space people without you I would not have survived the past 5 years. Thank you for always being there and for constantly supporting me in all my states.

Thank you for giving me the best memories.

I LOVE YOU GUYS.

I also want to dedicate this work to an inspiring person, teacher and mentor that helped me throughout my years and from whom I learned a lot, personally and professionally. Dr. Dalila Cherifi.

Finally, I would like to dedicate this work, to every students in the world, graduating this year in these critical "special" conditions.

WE MADE IT!

Amira

Dedication

I would like to dedicate this thesis to my beloved parents who have been a source of encouragement and inspiration to me throughout my life. Because of their unconditional love and prayers, I have the chance to complete this thesis.

Warm thanks go to my lovely aunt Djamila, whose constant encouragement, limitless giving and great sacrifice, helped me accomplish my degree. To my sisters Sabrina, Chahinez and my brother Rayan who always stood by my side and supported me, thank you for your continuous love and confidence.

I would also like to send my wholehearted thanks to my roommate and sister Nina for her unlimited support and care during these five years,

Thank you for all what we shared together!

Without forgetting a special person Abedlheq who was always here for me and helped me walk through my path to succeed and encouraged me to do more and bring out the best In myself.

Thank you!

Finally, many thanks to my friends and family members who were also a source for my aspirations ambitions.

Imene

Acknowledgement

First and foremost, our praises and thanks goes to Allah for his blessings during this critical time and the strengths to complete this research and dissertation successfully.

A special greeting goes to our professor and supervisor, Pr. Arab AZRAR for his continuous motivation, constant source of inspiration and patience all along this project. It was a great honor to work and study under his guidance and get the opportunity to do this work correctly. We could not have imagined having a better advisor for our master graduate project.

We would also like to thank all the workers and teachers who helped and assisted us during our five (5) year studies at the institute of Electrical and Electronic Engineering, Boumerdes. All the teachers who taught us to work under pressure and never give up during the hard and bad times.

At the end, we are grateful to anyone who has helped us physically, mentally or emotionally to successfully realize and finish this project during this sanitary critical situation.

Thank you!

Abstract

In this work, a four (4) elements linear microstrip patch antenna with a reduced mutual coupling degree to operate at the 2.45 GHz resonance frequency has been presented. Initially a single rectangular patch has been simulated using the CST MICROWAVE STUDIO printed on a FR4 dielectric material to resonate at 2.45 GHz with a reflection coefficient of -55 dB.

Then, the work is extended to a patch with a parasitic element coupled in the radiating edge of the pilot. The reduction of the mutual coupling is carried out by first spacing the patches; but the structure occupies more space. After that, curvatures and slots method is applied to reduce the occupied space. It is noted that the mutual coupling is amply reduced.

To quantify the mutual coupling reduction, the curvatures and slots method is further applied 4 elements linear antenna array. For purpose of comparison, the normal 4 elements linear antenna array is studied. The obtained results show that the mutual coupling has acceptable levels that is sufficient to maintain the array characteristics insensible to this effect.

Table of Contents

Chapter 2 Rectangular Patch Antenna with a Parasitic Element

Chapter 3: Linear Microstrip Array with Reduced Mutual Coupling

List of Figures

List of Tables

Chapter 1: Introduction to Antenna Arrays

1.1 Introduction

A device able to receive or transmit electromagnetic energy is called an antenna. Antennas have become ubiquitous devices and occupy a salient position in wireless system experienced the largest growth among industry systems. Antennas couple electromagnetic energy from one medium (space) to another medium as wire, coaxial cable, or waveguide. It also produces complex electromagnetic fields both near to and far from antennas. As a matter of fact, not all of the electromagnetic fields generated actually radiated into space, some of the fields remain in the vicinity of antenna and are viewed as reactive near fields; much the same way as inductor or capacitor is a reactive storage element in lumped element circuits [1]. There exist many forms of antennas which are characterized by specific feature and desirable applications in communication. Among the antenna forms we have wire, aperture, reflector, microstrip and array antenna. In the present work we will deal with linear microstrip array antenna.

1.2 Antenna array

In many applications it is necessary to design antennas with very directive characteristics (very high gains) to meet the demands of long distance communication. The radiation pattern of a single element is relatively wide, and each element provides low values of directivity, gain and bandwidth. This type (single element) of radiation is undesirable for point-to-point applications, and makes the design of antenna array overcome these shortcomings [1]

An antenna array is a group of antennas connected and arranged in a regular structure to form a single antenna that is able to produce strong radiation patterns. These antenna arrays are classified into linear, circular and planar arrays or 3-dimensional arrays depending on the positioning of the antenna elements [2]. The figure 1.1 illustrates these types.

The two basic types of antenna arrays are: uniform and non-uniform. Uniform antenna arrays are antennas with identical elements, where the input signal to each element consists of identical amplitudes and equal differential phase distribution. This

class of arrays has the narrowest main-lobe. On the other hand, Non-uniform array; with unequal amplitudes distribution, yields a more controlled side-lobe level due to many controlling inputs [4].

a) Linear array antenna

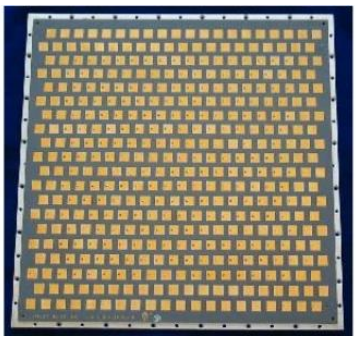

b) Planar microstrip array

Figure 1.1: Some types of antenna arrays [3]

1.2.1 Array factor

The gain of the antenna is increased using the principle of pattern multiplication. The later states that the total field of the array is equivalent to [2]

$$E(\text{total}) = [E\ (\text{single element at reference point})] \times [\text{array factor}]$$

For illustration, consider the N-element array shown in the figure 1.2. Let us assume all elements have identical amplitudes but each succeeding element has a ß progressive phase lead current excitation relative to the preceding one (ß represent the phase by which the current in each element leads the current of the preceding element)[2].

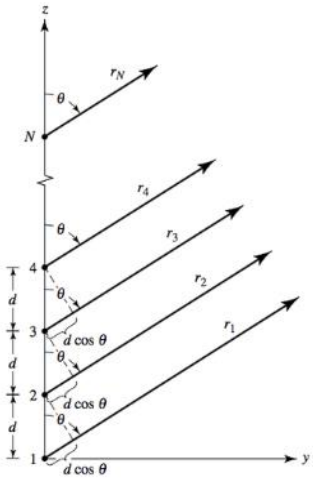

(a) Geometry

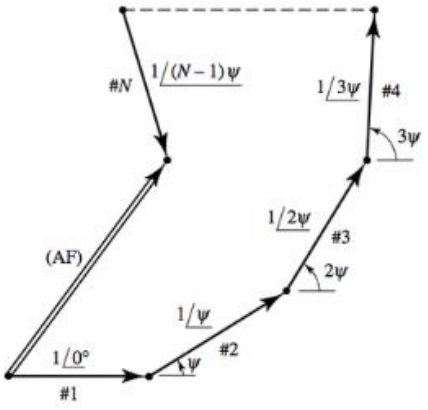

(b) Phasor diagram

Figure1.2: Far-field geometry and phasor diagram of N-element array of isotropic sources positioned along z-axis [4].

The discrete sources radiate individually but the pattern of the array is largely determined by the relative amplitude and phase of the excitation currents on each element and the geometric spacing apart of the elements. The array factor is given by [2]:

$$AF = 1 + e^{j(kd\cos\theta+\beta)} + e^{j2(kd\cos\theta+\beta)} + \ldots\ldots + e^{j(N-1)(kd\cos\theta+\beta)} \quad (1.1)$$

$$AF = \sum_{n=1}^{N} e^{j(n-1)(kdcos\theta+\beta)} \quad (1.2)$$

It can be written as:

$$AF = \sum_{n=1}^{N} e^{j(n-1)\psi} \quad (1.3)$$

Where: $\psi = kd\cos\theta + \beta$

k is the wave number given by 2Π/λ, d is the distance between the elements, θ is the angle of the main beam of antenna array and β is the progressive phase shift between individual elements.

Remark: For a uniform array the amplitudes are taken unity (amplitude = 1)

1.2.2 Feeding antenna arrays

Multiple antennas can be interconnected by means of a feed network to form an array and made to work for different purpose applications. The performance of the antenna array depends on our ability to feed the array elements with the appropriate feeding network. The most important feeding techniques are shown in the figure 1.3 and we can sum them as follow:

- **Parallel or corporate feed** network, where all the elements are feed in parallel from a single source. The power splitters are released using special RF power dividers, such as Wilkinson power dividers, or lossless combiners.
- **Series-fed** array, where antennas are feed in series from a common source.
- Both concepts, **series & corporate**, can be combined into a **hybrid feed**.

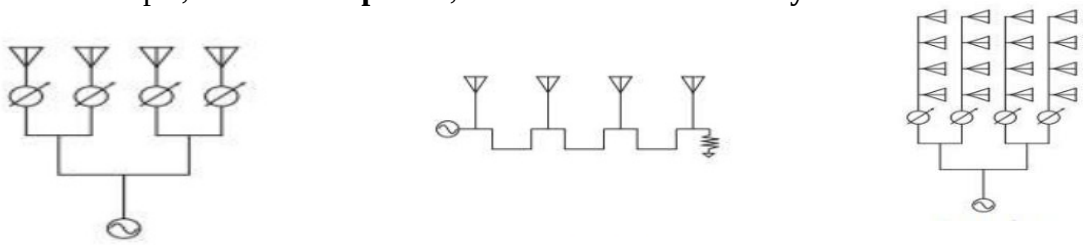

(a) Parallel / corporate feed **(b)** Series feed **(c)** Hybrid feed

Figure 1.3: Feeding array antenna techniques [5]

An Advantage of these arrays is that it implements something called frequency scanning, since the beam will scan with frequency [5].

1.2.2.1 Power divider

Microstrip power dividers/combiners are frequently used in the design of microwave components such as feeding network for antenna arrays or power amplifiers. The main goal of the power dividers is to control the power distribution of its outputs. In the last 50 years, several topologies of power dividers have been proposed. Amongst them we distinguish the Wilkinson power divider which is conventionally implemented with quarter-wave transmission lines. This structure provides a narrow bandwidth around a single center frequency. Recently, several modified Wilkinson structures have been introduced to principally extend its functionality to dual-band applications. We distinguish also the symmetric T-junction as equal power divider/combiner which is commonly used in the feed network of planar antenna arrays and Y-junction power divider. [6]

By definition, a -3dB power divider is ideally a passive lossless reciprocal three port device that divides power equally in magnitude and phase.

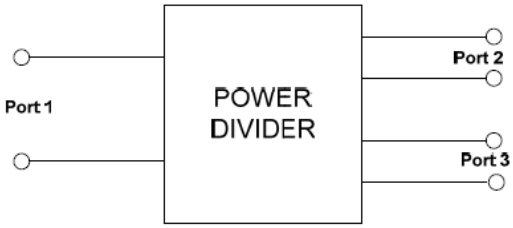

Figure 1.4: Block diagram power divider [2]

The general expression of the S-parameter matrix related this device is:

$$[S]= \begin{pmatrix} S_{11} & S_{12} & S_{13} \\ S_{21} & S_{22} & S_{23} \\ S_{31} & S_{32} & S_{33} \end{pmatrix} \quad (1.4)$$

Since all the three ports of this power divider are matched, $S_{ii} = 0$, and the network is reciprocal, $S_{ij} = S_{ji}$, the modified S-matrix can be written as:

$$[S]= \begin{pmatrix} 0 & S_{12} & S_{13} \\ S_{21} & 0 & S_{23} \\ S_{31} & S_{32} & 0 \end{pmatrix} \quad (1.5)$$

Also as the network is lossless then this matrix should be unitary and yields,

$$|S_{12}|^2 + |S_{13}|^2 = 1 \; and \; S_{23} \times S_{13}^* = 0 \quad (1.6a)$$

$$|S_{12}|^2 + |S_{23}|^2 = 1 \; and \; S_{13} \times S_{12}^* = 0 \quad (1.6b)$$

$$|S_{13}|^2 + |S_{23}|^2 = 1 \; and \; S_{12} \times S_{23}^* = 0 \tag{1.6c}$$

Considering the above equations, we see that the second column must have at least two out of three S parameters to be equal to zero. But if two of them were zero then one of the equations in the first column will be violated. Thus, we can conclude that it is impossible to satisfy all the three criteria of any power divider, such as, lossless, matched and reciprocal. Since relaxing anyone of them makes the other two achievable [2].

In this study, we will design a process of a four way array feeder network using Wilkinson type power divider. The Wilkinson divider can meet the ideal three-port network conditions (if it is matched at all ports) being lossless, reciprocal, matched. Therefore, the Wilkinson divider is the best choice and will be used in the optimized design of the corporate-fed network for the array [2].

The Wilkinson power divider is a three-port network that is lossless when the output ports are matched; where only reflected power is dissipated. Input power can be split into two or more in phase signals with the same amplitude. For a two-way Wilkinson divider using λ/4 impedance transformers having a characteristic impedance of $\sqrt{2}Z_0$ and a lumped isolation resistor of $2Z_0$ with all three ports matched, high isolation between the output ports is obtained. The design of an equal-split (3 dB) Wilkinson is often made in strip line or microstrip form; all designs considered in this work are microstrip, as shown below in Fig.(a). Whereas the equivalent transmission line circuit is shown in Fig. (b) [7].

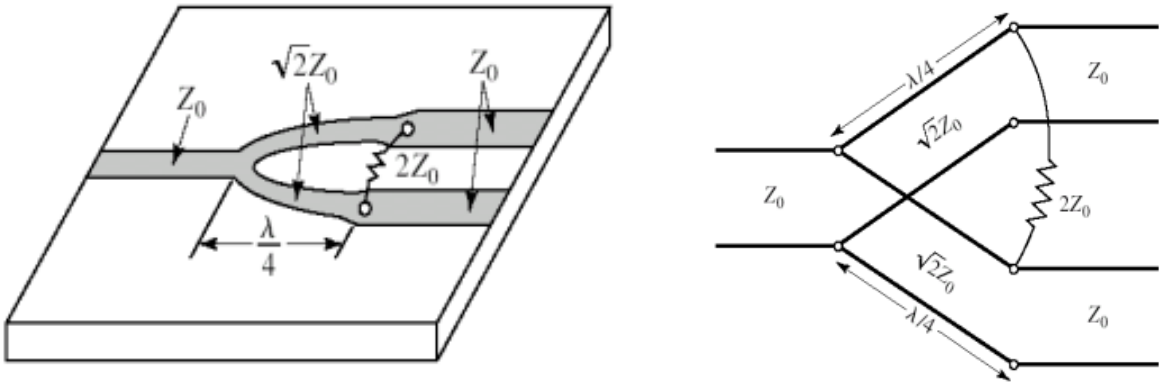

(a) **(b)**

Figure 1.5: The Wilkinson power divider [7]. (a) An equal-split Wilkinson power divider in microstrip form. (b) Equivalent transmission line circuit.

1.2.2.2 Phase shifter

Phase shifters are important elements for use in oscillators and phased array antenna systems, they are also the key element in the beam forming network. Phase shifters are components of an electronically scanned array that steers the antenna beam in the desired direction without physically repositioning the antenna. By definition, they are a two ports network where output signal may adjust to have some desired phase relationship to the input signal by using a control signal [2]

Phase shifters are classified into digital and analog types as show in figure1.6.

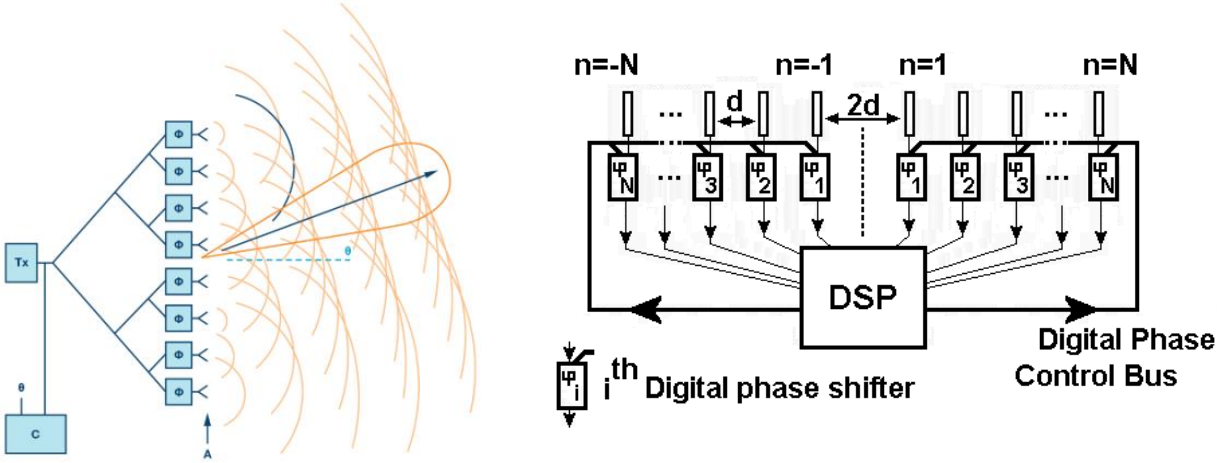

(a) Analog phase shifter [8] **(b)** digital phase shifter [9]

Figure 1.6: Diagram of phased array showing both analog and digital

Remark: While designing an array the feed point and the distance between each element are kept constant in order to provide equal phase excitation.

1.2.3 Mutual Coupling

Mutual coupling is an unavoidable phenomenon in multi-antenna systems, which degrade the system performance. In antenna array system when two antennas are placed close to each other, interaction takes place between them. This not only increases the transmission coefficient but also distorting the radiation pattern, and deteriorates the signal plus interference to noise ratio [10]

In other words, in a phased array, the electromagnetic (EM) characteristics of a particular antenna element influence the other elements and are themselves influenced by the elements in their proximity. This inter-element influence or mutual coupling between the antennas is dependent on various factors, namely, number and type of antenna

elements (A), inter-element spacing, relative orientation of elements, radiation characteristics of the radiators, scan angle, bandwidth, direction of arrival (DOA) of the incident signals, and the components of the feed network that is, phase shifters (P) and couplers (C)[11].

Several researchers have studied the effect of mutual coupling on different types of adaptive arrays. These include Yagi array, power inversion array, circular array of isotropic elements and semi-circular array of printed dipoles, microstrip patch antenna arrays [11]. The effect of mutual coupling on the array parameters such as antenna impedance and steering vector, which further affects the radiation pattern, resolution and interference suppression ability cannot be completely ceased but it can only be reduced using the different techniques .

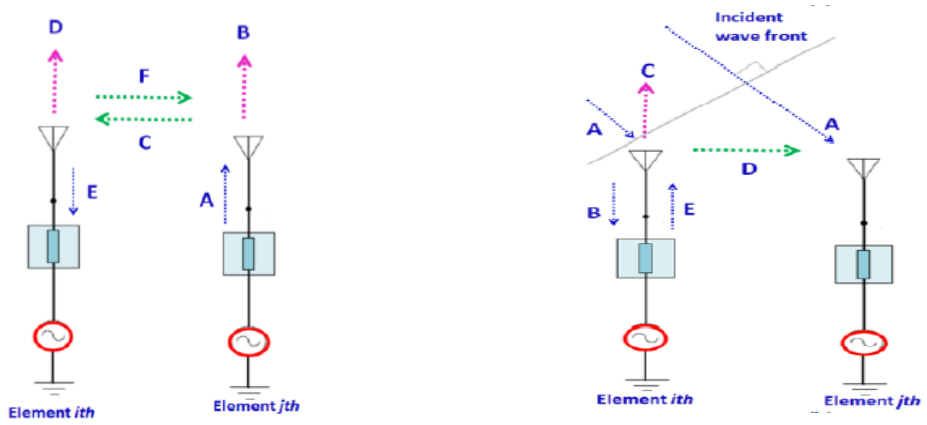

(a) **(b)**

Figure 1.7: Diagram of mutual coupling mechanism.
(a) Transmitting mode and (b) receiving mode [12]

1.3 Mutual Coupling Reduction Techniques in Microstrip Array

Mutual coupling is an undesirable electromagnetic phenomenon which degrades the system performance and exists in mainly all the antenna arrays. Over the past years, several methods have been proposed and provided to reduce the mutual coupling between radiating elements in antenna arrays. Some of the most important techniques to reduce mutual coupling are summarized in figure 1.8.

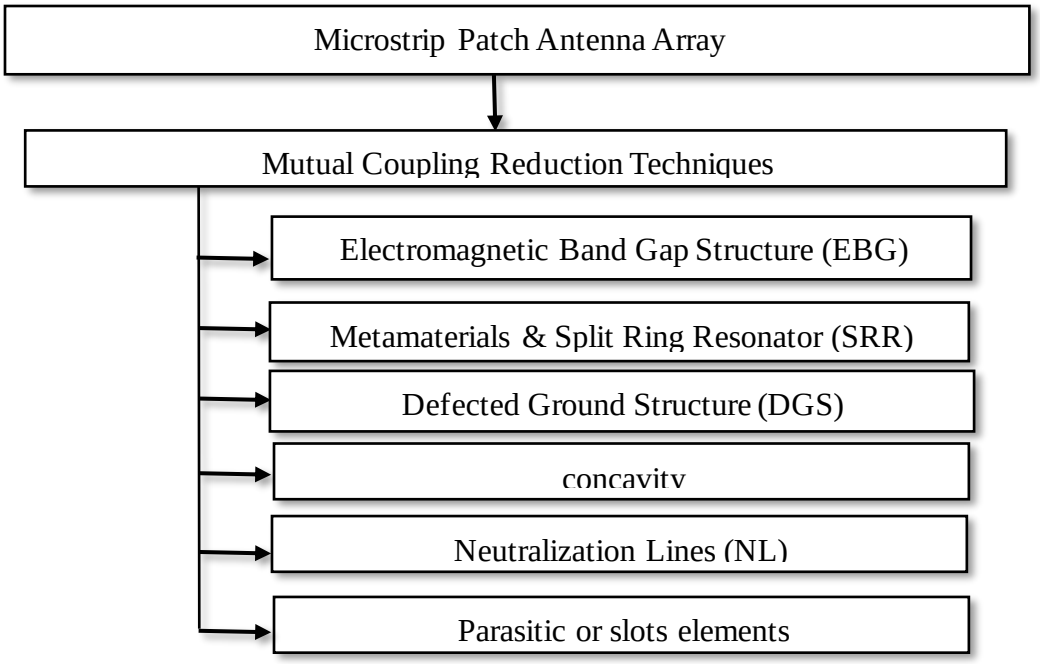

Figure1.8: Mutual coupling reduction techniques [12]

1.3.1 Electromagnetic Band Gap Structure (EBG)

One of the methods that provide substantial solution to the disadvantages of microstrip antennas and arrays as the reduction of mutual coupling is Electromagnetic Band Gap (EBG) structures. EBG structures are defined as manmade periodic structures that prevent or stop the propagation of electromagnetic waves for a particular band of frequencies for all incident angles and polarization states. EBG structures can be dielectric materials or metallic conductors [13]. Different EBG structures are shown in figure 1.9 and they are:

- Three-, two-, and one-dimensional (3D, 2D, and 1D) EBG.
- Mushroom and uniplanar EBG, and their successive advancement [14].

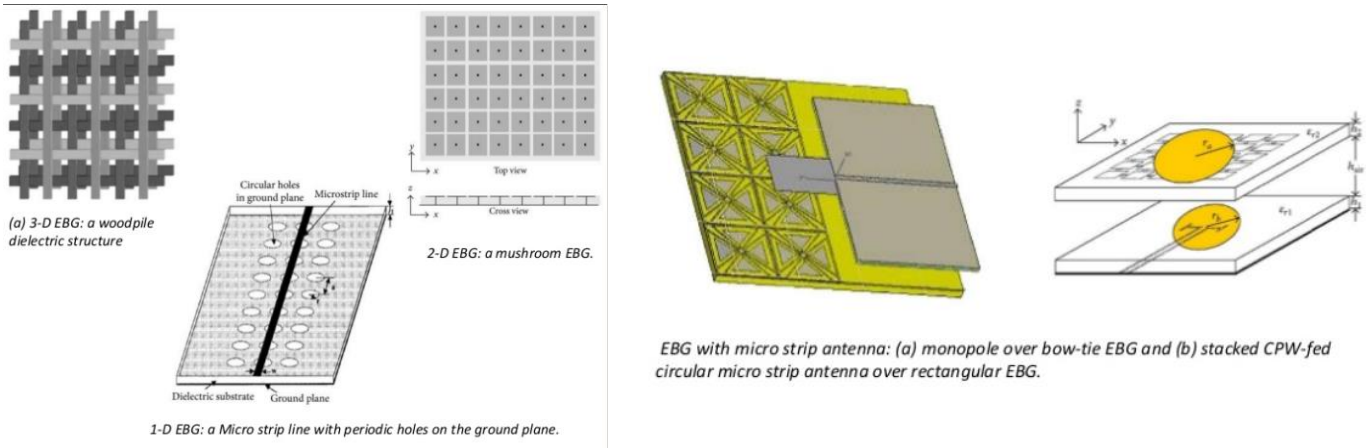

Figure 1.9: Different types of EBG structures [14]

The two dimensional and one dimensional structures are preferred over the three dimensional structures as the three dimensional structures are complicated to design and implement [13].

1.3.2 Metamaterial

The meta-materials are artificial composites, homogeneous with electromagnetic properties not found in nature [16]. They have negative relative permittivity and/ or permeability, where these two properties will determine how a material will interact with electromagnetic radiation [15].

Spiral resonator acting as metamaterial (SR) presented is one of popular techniques which is proposed as a solution to reduce the mutual coupling in a microstrip array antennas (Figure 1.10). This structure can reduce the mutual coupling of about 5.5 dB [13].

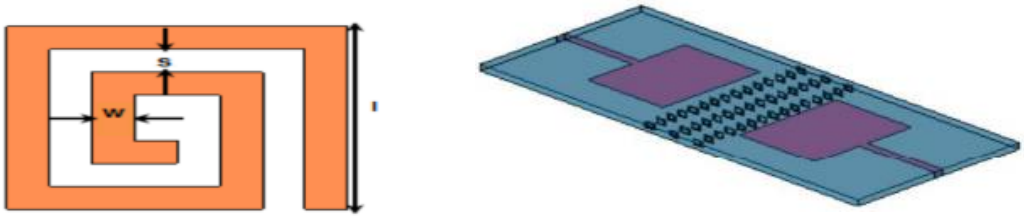

(a) **(b)**

Figure 1.10: (a) A unit cell of periodic Structure, **(b)** view of array antenna with SR structure for 3 rows [16]

Complementary Split Ring Resonator (CSRRs) are usually periodic configurations of metallic ring, shunt strip or capacitive gap used to perform filtering as well as isolation improvements function and lower mutual coupling [12]. The idea is to place three etched spiral resonators in the ground plane of the two antennas, between their coaxial probes excitations, as shown in figure 1.11 (b).

(a) **(b)**

Figure 1.11: (a) Complementary split spiral Resonator, **(b)** The proposed microstrip antenna (CSSR) unit cell [16].

1.3.3. Defected ground structures (DGS)

DGS is an etched periodic or non-periodic cascades configuration defect in ground of a planar transmission line (as microstrip…) which disturbs the shield current distribution in the ground plane cause of the defect in the ground [17].

Coupling between adjacent antenna elements which caused by ground currents can be reduced by applying modifications to the ground plane. Ground plane modifications such as cutting slits or other shapes, as shown in figure 1.12. They work as band stop filter for the coupling fields generated by ground currents. Most commonly the defected ground structures are placed beneath the transmission line which reduces the effect of electromagnetic fields around the defect [18].

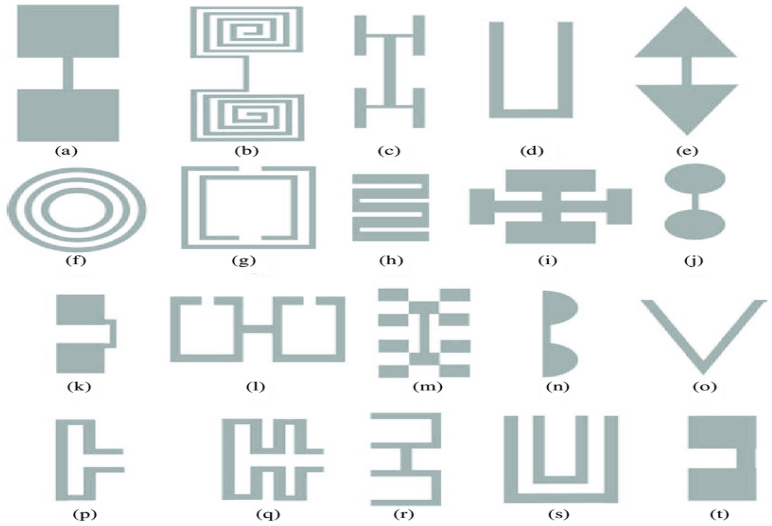

Figure 1.12: Various DGS geometries
(a) dumbbell-shaped, **(b)** spiral-shaped, **(c)** H-shaped, **(d)** U-shaped, **(e)** arrow head dumbbell, **(f)** concentric ring shaped, **(g)** split-ring resonators, **(h)** interdigital, **(i)** cross-shaped, **(j)** circular head dumbbell, **(k)** square head connected with U slots, **(l)** open loop dumbbell, **(m)** fractal, **(n)** half-circle, **(o)** V-shaped, **(p)** L-shaped, **(q)** meander lines, **(r)** U-head dumbbell, **(s)** double equilateral U, **(t)** square slots connected with narrow slot at edge [19].

1.3.4 Concavity

Another important solution to reduce mutual coupling in microstrip antenna array, is making concavity on the patch in horizontal, vertical or both sides as shown in figure 1.13. Having a shape cute on the radiating edges of the antenna will help us reduce the mutual coupling effect and enhance the capacity of the antenna array. [20]

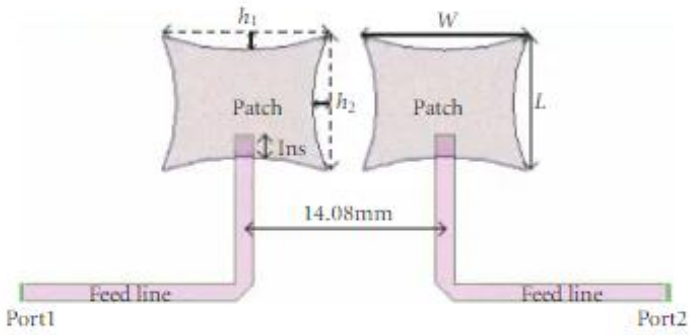

Figure 1.13: Array of concave rectangular antennas [20]

1.3.5 Neutralization Lines (NL)

Neutralization lines are also effective in reducing the coupling. In neutralization technique current taken from one element is fed to other element with reversed phase using a transmission line of suitable length to minimize the coupled currents with second element as shown in figure 1.14. The complication in this technique is, to select a proper location of maximum current to be picked up and to manage proper length of neutralization line to reverse the phase of that current with in limited space available. It takes very detailed analysis of current distribution and associated phase on antenna. Also these line are suitable for narrow band antennas, they are not as effective for wide bandwidth. Neutralization lines are not always straight lines; they can sometimes look like decoupling structures and can act as both a decoupling network and a neutralization line [18]

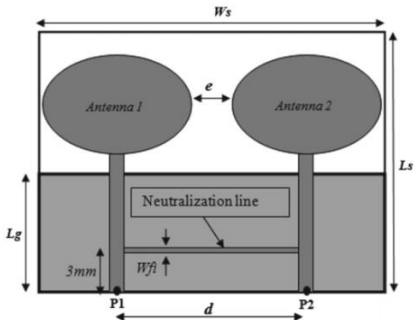

Figure 1.14: Geometry of Elliptical multi-antennas with neutralization [21]

1.3.6 Parasitic element

They are the elements which are placed near antenna elements or between two elements, in case of antenna array systems to minimize coupling as illustrated in figure 1.15. They also create opposite coupling fields between antenna elements to counter coupling fields between antennas. Parasitic elements are not actually connected to antenna elements, they are placed near them. They are advantageous as they can be designed for various purposes

such as to control bandwidth along with decoupling. They can be composed of resonators or stubs with both floating and/or shorted arrangements [18].

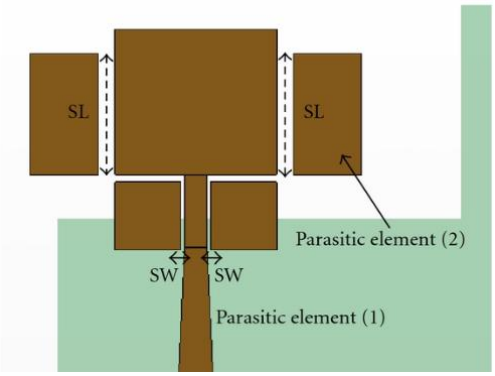

Figure 1.15: Planar antenna with parasitic elements [22]

1.3.7 Slots: They are considered as another basic radiating element. It is realized by removing a small area of metal from an infinite ground plane or patch. For a practical design, however, the ground plane may be finite but large in size. The open area, or the 'slot,' can be of any shape and size, but is shown in the figure below to be rectangular, as is often done for simplicity. A slot antenna may be excited by applying a voltage source across the slot (figure 1.16) [22].

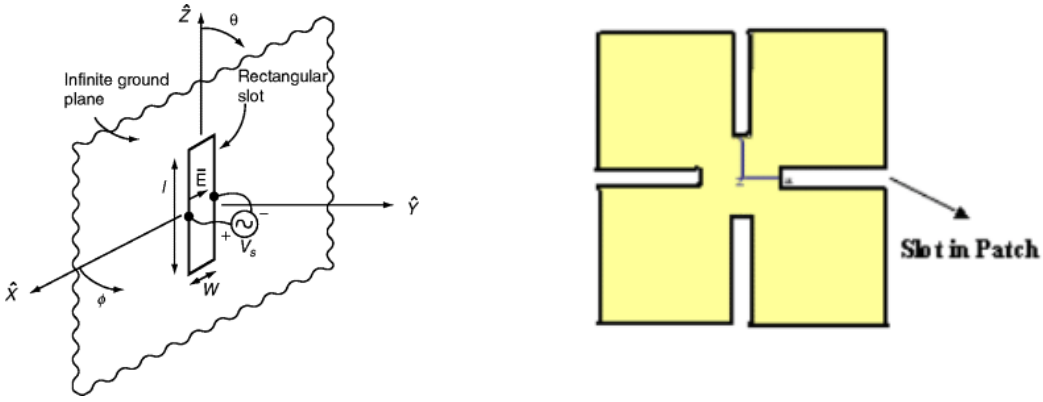

Figure 1.16: A Slot Antenna produced by a rectangular opening at the center of an infinite ground plane [23-24]

1.4 Microstrip Antennas Overview

1.4.1 Basic Structure of Microstrip Antenna

The basic design of the microstrip patch antenna consists of other Radiating Metallic Patch on one side of dielectric Substrate, Ground Plane on the side and all printed directly onto a circuit board as shown in figure 1.17.

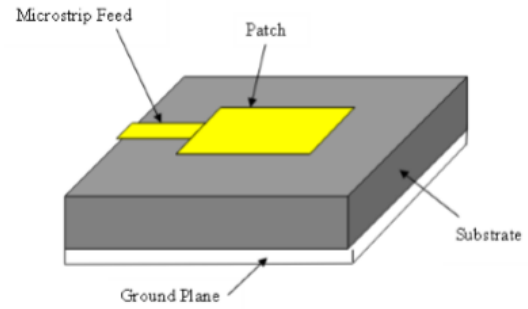

Figure 1.17: Microstrip patch antenna configuration [25]

- The metallic patch is normally made of thin copper foil plated with corrosion resistive metal such as gold, tin or nickel. There exists different shape of patches, and the most common ones are the rectangular and circular patches.
- The substrate allows isolating both conductive planes and characterized by permittivity. The typical range for dielectric constant of the substrate being used is $2.2 \leq \varepsilon_r \leq 12$ [25].
- The Ground plane is a conductor situated below the circuit on which is placed the substrate.

1.4.2 Radiation mechanism of microstrip antenna

Radiation from Microstrip antenna can be understood by considering the Figure 1.18 that shows a cutting of the Microstrip antenna where different regions may be distinguished according to the type of electromagnetic field [26].

In region (A) of the substrate between the two conductors, we find a concentration of the electromagnetic field. The lower the frequency of operation the higher this concentration is. Thus, there is propagation without radiation and the resulted structure is a transmission line or of its derivatives (junction, bend, etc) [26].

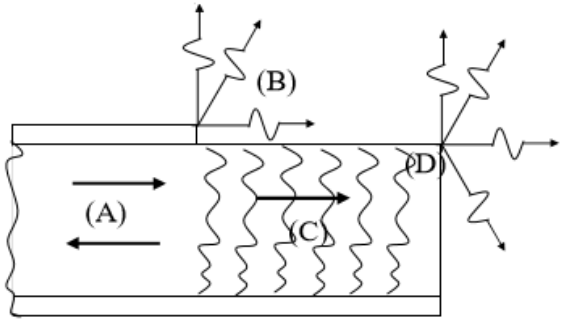

Figure 1.18: Configuration of principle regions of a microstrip antenna [26]

So the structure presents a behavior of an antenna. Since the surface currents are circulating essentially on the interior face of the above conductor, the radiation appears to be emitted at the ends (discontinuities). At this level of the structure, there is, in fact, a scattered field that is responsible of radiation [26]

1.4.3 Feeding Techniques

Microstrip patch antennas can be fed by a variety of method, these methods can be categorized into two main feeding methods as shown in figure 1.19 [27]:

- Contacting (Direct) method: the RF power is fed directly to the radiating patch using a connecting element.
- Non-contacting (Indirect) method: the electromagnetic field coupling is done to transfer power between the microstrip line and the radiating patch.

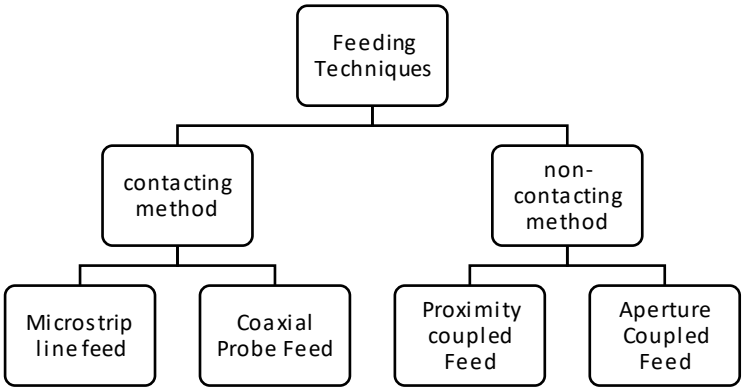

Figure 1.19: Feeding Techniques methods

i) Microstrip Line feed

A conducting strip is connected to the edge of the patch as illustrated by figure 1.20. The feed can be etched on the substrate. This method is simple, easy to fabricate and it can be etched on same substrate. But it gives undesired radiation [29].

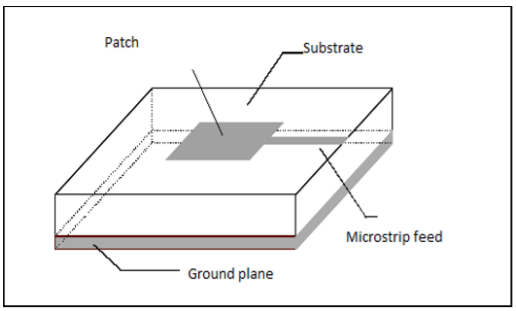

Figure 1.20: Microstrip line technique [28]

ii) Coaxial probe feed

The inner conductor of the coaxial connector extends through the dielectric and is soldered to the radiating patch, while the outer conductor is connected to the ground plane as shown in figure 1.21 below. The feed can be placed at any desired location with low spurious radiation. However, it results in narrow bandwidth and the method is difficult to model [29].

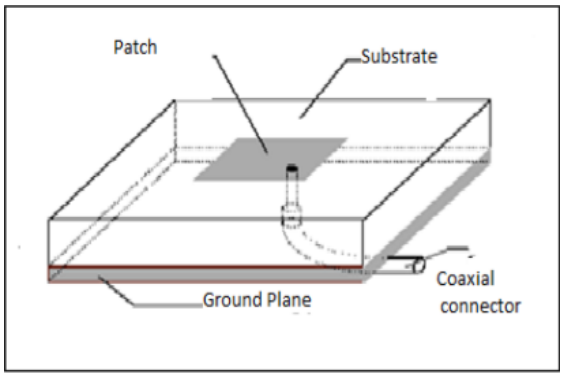

Figure 1.21: Coaxial Probe Feed [28]

iii) Aperture Coupled Feed

Coupling between the patch and feed line is made through a slot or an aperture in the ground plane as depicted in figure 1.22. This method eliminates spurious radiation. The realization process of this method is difficult [29].

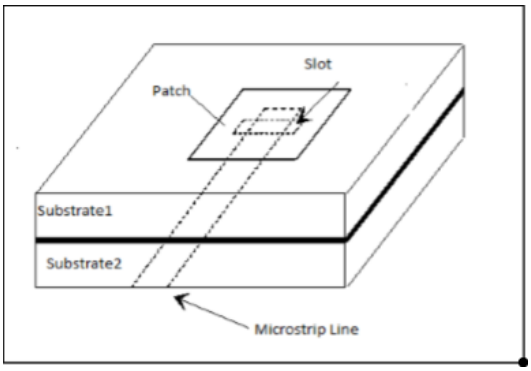

Figure 1.22: Aperture coupled feed [28]

iv) Proximity Coupled Feed

Two dielectric substrates are used such that the feed line is between the two substrates and the radiating patch is on top of the upper substrate as shown in the next figure, 1.23. As the previous method, it eliminates spurious radiation but the thickness of antenna increases [29].

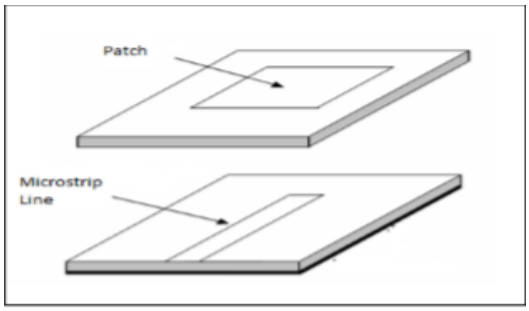

Figure 1.23: Proximity coupled Feed [28]

1.4.4 Methods of analysis

The most well-known methods for the analysis of Microstrip patch antennas (figure 1.24) are divided into two groups of methods; ***(i)*** Analytical methods based on equivalent magnetic current distribution around the patch edges and ***(ii)*** Numerical methods based on the electric current distribution on the patch conductor and the ground plane [26].

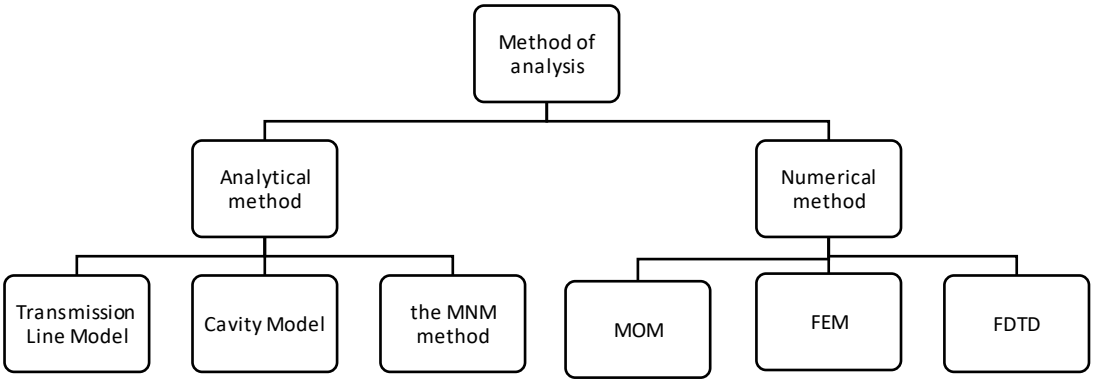

Figure 1.24: Method of analysis of a Microstrip Antenna.

1.4.5 Advantages & Disadvantages

1.4.5.1 Advantages

- Low weight, low profile planar configuration and low volume.
- Simple to design and easy to modify according to needs.
- Low cost of fabrication and ease of manufacturing.
- They allow for dual- and triple-frequency operations.
- They can be made compact for use in personal mobile communication.

1.4.5.2 Disadvantages

- Narrow bandwidth.
- Lower efficiency and gain.

- Low power-handling capability.
- Extraneous radiation from feeds and junctions.
- Poor end fire radiator except tapered slot antennas.

However, because of the advantage of a single microstrip antenna, the usage of microstrip array antennas is quickly increasing…

1.5 Microstrip Array

Microstrip antennas are used in arrays as well as single elements. However, Microstrip arrays are capable of radiating efficiently only over a narrow band of frequencies and hence they can operate only at the low power levels of waveguide. Using a single element is difficult to increase the directivity and perform various functions, such as pattern beam forming, smart antennas, electronic scanning radars, missiles, military and satellite communication [30].

In the microstrip array, elements can be fed by a single line called series feed or by multiple lines called corporate-feed network:

A. Series feed network

By connecting elements with high impedance transmission line and feeding the power at the first element Series feed microstrip array can be formed (figure 1.25). As the feed arrangement is compact the line losses associated with this type of array are lower than those of the corporate feed type [30].

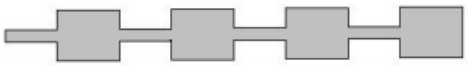

Figure 1.25: Series feed of a microstrip array [30]

The drawback of series feed arrays is the large variation of the impedance and beam pointing direction over a band of frequencies [30].

B. Corporate feed network

The corporate feed (figure 1.26) networks are used to provide power splits of the order 2n (i.e. n = 2; 4; 8; 16; etc.,) which can be accomplished by using either the tapered lines or by using quarter wavelength impedance transformers.

Corporate feed arrays are general and versatile in nature. This particular method has more control of the feed of each element and therefore, it is ideal for scanning phased arrays. Accordingly, providing better directivity as well as radiation efficiency and hence

reducing the beam fluctuations over a band of frequencies compared to the series feed array [30].

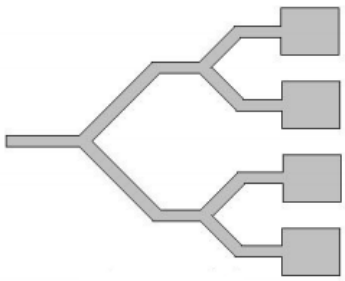

Figure 1.26: Corporate feed of microstrip antenna array [30]

Remark: The phase shifter is used to control the phase of each element while amplitude can be adjusted by using either the amplifiers or the attenuators [30].

1.6 Conclusion

In this chapter, array antennas are introduced with emphasize on Microstrip Antennas type that will be used in this work throughout the next chapters. The phenomenon of Mutual coupling is also investigated and its reduction techniques are presented and analyzed. Most of these techniques need additional material or space occupation to proceed which is a drawback in the microstrip antenna array applications.

Therefore, Concavity and slotting methods are the most suitable ones to apply in our work, where reducing mutual coupling by fringing effects will help to prevent the wave propagation to the nearby antennas that will grasp the power of the wave and less power is radiated to the desired direction. A change in the amount of concavity in length or width results in an alteration in the resonant frequency of antenna. As a result, the patch impedance is distorted and must be corrected by changing the other antenna parameters, such as the patch width and the excitation point. This technique is also applied with a very small distance between the radiating patches compared to the operating wavelength and will not affect the radiation patterns as will be shown in the next chapters. Furthermore, creating concavity in the patches is an effective solution to reduce the mutual coupling and return loss in the microstrip antenna array, as well as enhancing its capacity and efficiency.

Chapter 2: Rectangular Patch Antenna with a Parasitic Element

2.1 Introduction

Microstrip Antenna Array are introduced and discussed in the previous chapter, as well as the mutual coupling reduction techniques by emphasizing on concavity which is the one chosen to apply in our project. A rectangular shaped microstrip patch antenna will be designed to operate at 2.45 GHz using transmission line model, excited using a coaxial probe feed as shown in [31]. [31] Will be used as a reference to this part of our work and the simulation process is done using CST.

2.2 Rectangular microstrip patch antenna

The rectangular shape is probably the most used microstrip patch antenna for its simplicity as it is characterized by a Length (L), Width (W) thickness (t) all on a substrate of thickness (h) as shown in the figure 2.1.

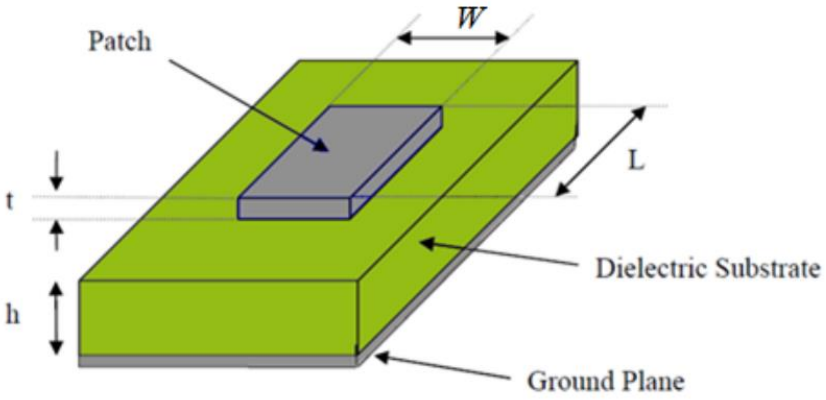

Figure 2.1: A rectangular microstrip antenna [32]

2.2.1 Antenna Parameters and Characteristics

Each antenna is characterized by fundamental parameters for a specific application where some of them are interrelated and not all of them need to be specified for complete description of the antenna performance. Among those parameters we can mention the most important ones in our work.

2.2.1.1 Input Impedance (Z_{in})

The Input Impedance is defined as the impedance presented by an antenna at its terminal, in other words it is the ratio of the voltage to the current at the pair of terminals or ratio

of the appropriate components of the electric to magnetic fields at a point [31]. The equation (2.1) illustrates this in a complex form where the real part is input resistance R_{in} and the imaginary part representing the input reactance X_{in}.

$$Z_{in} = R_{in} + jX_{in} \tag{2.1}$$

Z_{in} can also be defined as the impedance view from the feed line and it is given by the equation (2.2)

$$Z_{in} = Z_0 \frac{1+S_{11}}{1-S_{11}} \tag{2.2}$$

Where: Z_0 is the characteristics impedance.

S_{11} is the input reflection coefficient.

2.2.1.2 Return Loss (S_{11})

Return loss is one of the important parameter in antenna testing. Return loss, also stared as the S_{11} of the S-parameters, is the power of the reflected signal in a transmission line. It can be calculated by equation (2.3) and it is given in (dB) [33]:

$$RL(dB) = 10\log\left(\frac{P_r}{P_{in}}\right) = 20\log\left|\frac{Z_{in}-Z_0}{Z_{in}+Z_0}\right| \tag{2.3}$$

P_r: Power Reflected back from the antenna.

P_{in}: Source incident power of the antenna.

To obtain a satisfactory matching the return loss should be -10 dB and for an ideal one -30dB. The less the return loss, the better the matching and the less power is reflected back.

2.2.1.3 Voltage Standing Wave Ratio (VSWR)

Another way to see how much the system is matched, VSWR is the ratio between the maximum voltage V_{max} and minimum voltage V_{min} in the transmission line, and can be defined as follows [33]:

$$VSWR = \frac{Vmax}{Vmin} = \frac{1+\rho}{1-\rho} \tag{2.4}$$

Where ρ is the magnitude of the reflection coefficient | Γ | also known as S_{11} or Return loss.

and

$$\Gamma = \frac{Z_{in}-Z_0}{Z_{in}+Z_0} \tag{2.5}$$

Where Z_0 is the characteristics impedance and it is set to 50 ohm for the coaxial cable.

2.2.1.4 Bandwidth (BW)

Bandwidth is defined from the frequency limits at which the standing-wave ratio (SWR) reaches a maximum threshold, assuming that the feeding transmission line that connects to the patch is perfectly matched at the resonance frequency (i.e., $Z_0 = R$, if we neglect the effects of the probe inductance) [4]. The bandwidth is thus defined as:

$$BW = \frac{f_H - f_L}{f_r} \tag{2-6}$$

Where:

f_H and f_L : The high and low frequencies on either side of the resonance frequency at which VSWR = 2, or S_{11} = -10 dB with S being a prescribed value.

f_r: The impedance resonance frequency of the patch. An antenna is said to be broadband if its BW is 2 or higher, otherwise it is said to be narrowband.

2.2.1.5 Radiation Pattern

The antenna pattern can be defined as "the mathematical function or graphical representation of the radiation properties as a function of space coordinates". In most cases, the radiation pattern is determined in the far-field region and is represented as a function of the directional coordinates in a 2D or 3D pattern. It can represent several properties such as gain, power flux density, electric field, radiation intensity, field strength, directivity, phase or polarization [4].

- The tridimensional radiation patterns is measured in spherical coordinates, function of (θ, ϕ, r), the x-z plane ($\varphi = 0°$) usually indicates the elevation plane (E-plane), while the x-y plane ($\theta = 90°$) indicates the azimuth plane (H-plane).
- The bi-dimensional radiation pattern represents a cut of the 3D radiation pattern, for given angles $\theta = \theta_0$ or $\phi = \phi_0$

2.2.2 Design of a rectangular microstrip patch antenna

The considered antenna in our project, has the same specifications as the one in [31] where all the dimensions have already been calculated and the parameters of the dielectric material specified

2.2.2.1 Substrate and Frequency Specifications

The dielectric material available in our laboratory is the FR4 glass epoxy and its parameters are shown in table 2.1. The dielectric materiel will be used as the dielectric substrate in our antenna operating at 2.45 GHz.

Table 2.1: *Parameters of the dielectric substrate for the rectangular patch antenna*

Dielectric Substrate	Thickness (**h**)	Loss tangent (**tanδ**)	Relative permittivity (**εr**)
	1.6 mm	0.017	4.3

2.2.2.2 Calculated dimensions of the antenna

Rectangular patch has four (4) parameters that should be calculated to obtain its Width (W) and Length (L). [4]

a) Width (W)

$$W = \frac{C}{2f_r}\sqrt{\frac{2}{\varepsilon_r+1}} \tag{2.7}$$

b) Effective Dielectric constant ε_{reff}

$$\varepsilon_{eff} = \frac{\varepsilon_r+1}{2} + \frac{\varepsilon_r-1}{2}\frac{1}{\sqrt{\left[1+12\frac{h}{W}\right]}} \tag{2.8}$$

c) ΔL

$$\Delta L = h\frac{(\varepsilon_{eff}+0.3)\left(\frac{W}{h}+0.264\right)}{(\varepsilon_{eff}-0.258)\left(\frac{W}{h}+0.8\right)} \tag{2.9}$$

d) Length (L)

$$L = \frac{C}{2f_r\sqrt{\varepsilon eff}} - 2\Delta L \qquad \text{C is the free space light's speed} \tag{2.10}$$

Using (2.7)-(2.10) we obtain: **W = 37.61 mm** and **L = 29.15 mm**

W and L are responsible of controlling the input impedance and the radiation pattern and affecting the operating frequency respectively.

2.2.3 Design procedure and Simulation results

2.2.3.1 Design Procedure

To operate at exactly 2.45 GHz and achieve the exact matching, some adjustments are made in the antenna's width and length as well as for the feeding point compared to the results of [31]. This is due to the difference in the software, mainly because IE3D has an infinite ground and CST a finite one where it has to be at least 2 times the patch dimensions.

After several simulations attempts and according to CST, the dimensions that produce the exact resonance frequency, 2.45 GHz and a satisfactory matching between the input impedance and the probe characteristics impedance (usually 50 ohm) are summarized in the table 2.4 and shown in the figure 2.2. In our case, we used a discrete port to feed our antenna, which is in CST equivalent to 50 ohm. The Feed port is varied at different coordinates across the *x*-axis (Xp) and not very far from 6.562 in [31] while the *y* coordinates are Yp = 0. Finally, we fixed the point to Xp = 6.49 mm that gave us the 50 ohm impedance.

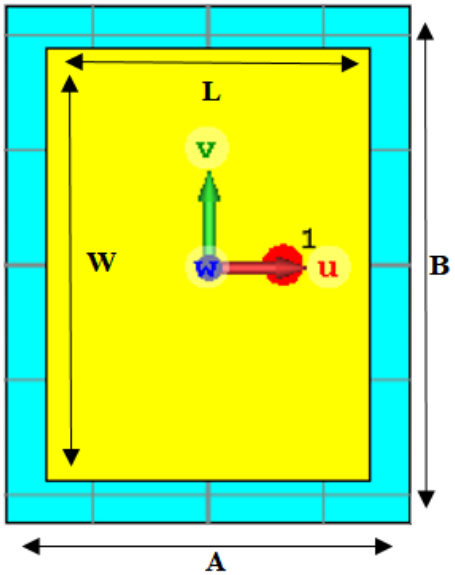

Figure 2.2: A rectangular patch antenna with optimized dimensions

Table 2.2: *Dimensions of the ground*

Ground Dimensions	Width (**B**)	length (**A**)	Depth (**T**)
	117 mm	75 mm	0.035 mm

Table2.3: *Dimensions of the Substrate*

Substrate Dimensions	Width (**B**)	length (**A**)	Depth (**h**)
	117mm	75mm	1.6 mm

Table 2.4: *Dimensions of the Patch*

Patch Dimensions	Width (**W**)	Length (**L**)	Excitation Point (**Xp**)	Depth(**T**)
	37.6 mm	28.16 mm	(6.49,0)	0.035mm

2.2.3.4 Simulation results

i) **Input reflection coefficient and Bandwidth**

From CST software we obtained the graph of the reflection coefficient of our antenna shown in figure 2.3 and we can get:

The magnitude is about -55 dB which is much less than the -10 dB matching value, which represents an ideal matching for our patch. The patch resonates at exactly 2.45 GHz. The Upper and Lower frequencies to obtain the bandwidth of the antenna using the equation (2-6) and operating at -10 dB as shown in Figure 2.4

$$BW = \frac{2.4758 - 2.4242}{2.45} \times 100 = 2.147\%$$

This means that our antenna is narrowband.

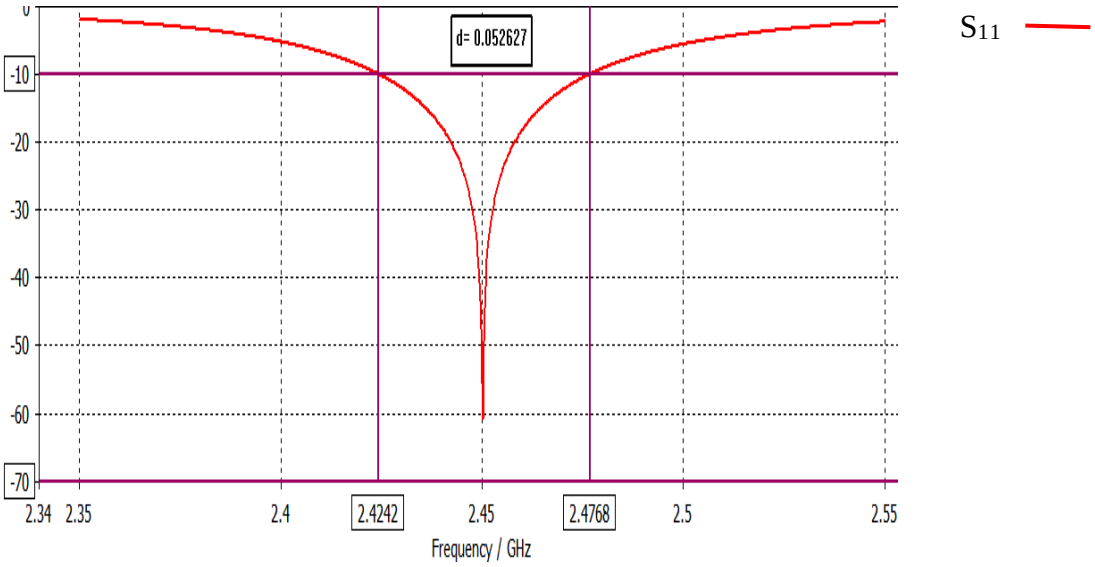

Figure 2.3: Input reflection coefficient of the rectangular patch antenna

Another way to conclude the matching and the bandwidth is by observing the VSWR of the desired antenna. The figure 2.4 shows the VSWR. From that figure, we can see that the VSWR = 1 at the resonant frequency; which leads to a good matching of our antenna.

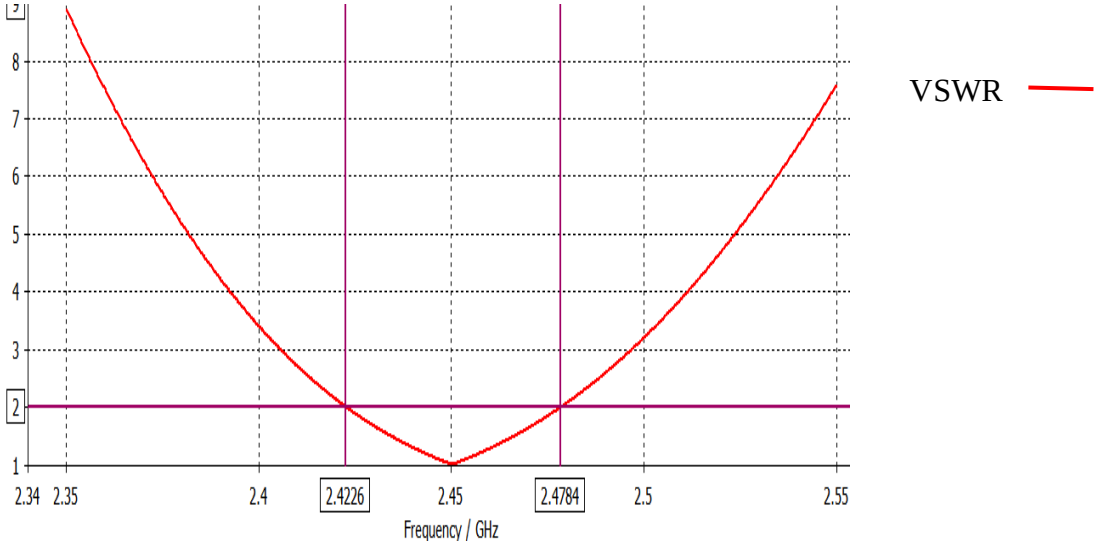

Figure 2.4: VSWR of the Rectangular patch antenna

ii) Input impedance

The input impedance at 2.45 GHz of the patch is 50 ohm and 0 for its real and imaginary parts, respectively as shown in Figure 2.5.

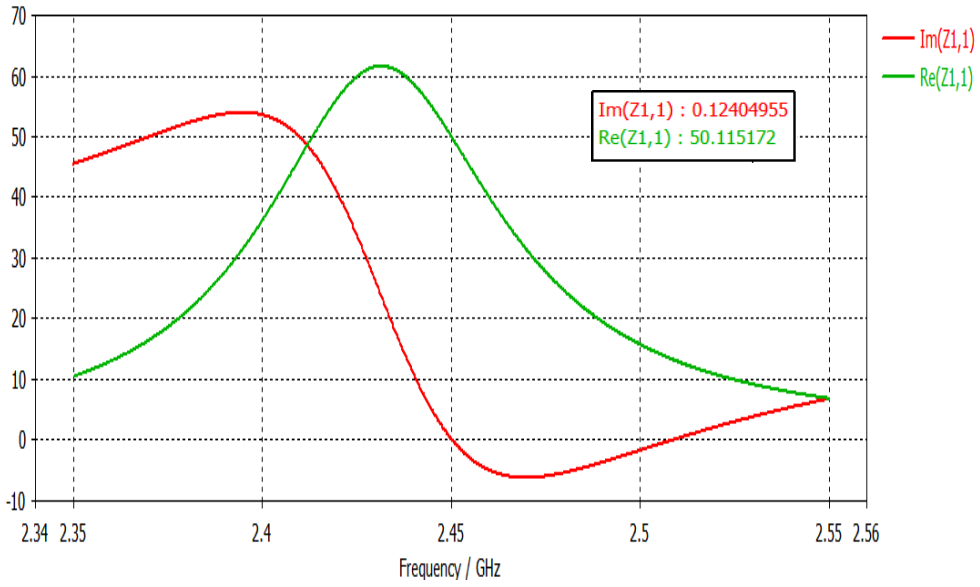

Figure 2.5: Real and Imaginary part of the rectangular patch input impedance

iii) Current Distribution

The current distribution is drawn at frequency of 2.45 GHz as shown in the figure 2.6. We can observe that the current is close to maximum in the center and around the feed port and minimum at the edges. The Figure also shows that the current distribution is a sort of arrows flowing in the x-axis showing the linear *x*-polarization.

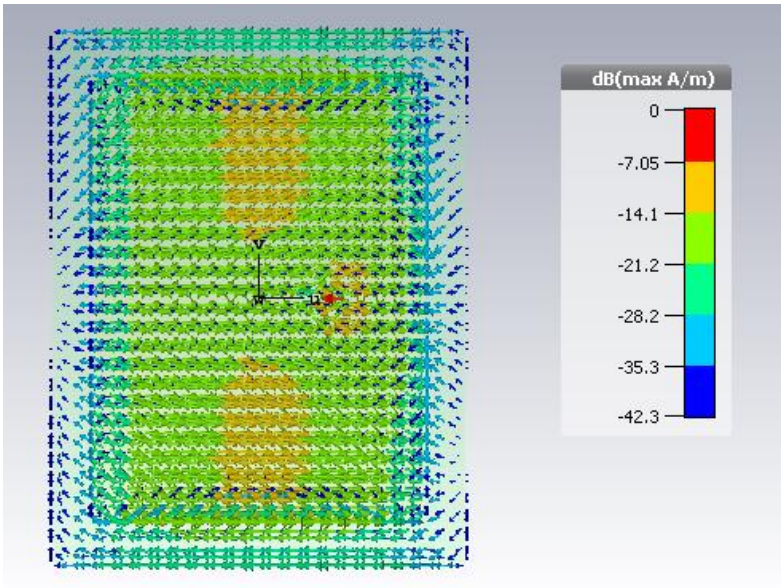

Figure 2.6: Current distribution of the rectangular patch antenna at 2.45 GHz

iv) Radiation Pattern

a) 2D-Respresentation of Radiation field patterns

The Radiation field patterns are shown in a 2D representation of the far field patterns in figure 2.7 a and b. They are presented in the polar form with the dBi as a scale.It is evident that the maximum radiation is perpendicular to the ground plane of the antenna ($\theta = 0\circ$) in the two planes (**$\phi = 0°$** and **$\phi = 90°$)**, with a gain of 3 dBi.

An antenna is said to have good polarization purity if the level of the cross polarization component, is at least 20 dB lower than the co-polarization component. The Ludwig definition of the 02 components of an antenna polarized along the x axis gives [34]:

$$\begin{bmatrix} E_{co} \\ E_{cross} \end{bmatrix} = \begin{bmatrix} +\cos(\Phi) & -\sin(\Phi) \\ +\sin(\Phi) & +\cos(\Phi) \end{bmatrix} \begin{bmatrix} E_{\theta} \\ E_{\Phi} \end{bmatrix} \tag{2.11}$$

- E-plane: $\phi = 0 \Rightarrow E_{co} = E_{\theta}$ & $E_{cross} = E_{\Phi}$. Both E-plane's co and cross polar components are shown in figure 2.7a.
- H-plane: $\phi = \frac{\pi}{2} \Rightarrow E_{co} = -E_{\Phi}$ & $E_{cross} = E_{\theta}$. Both H-plane's co and cross polar components are shown in figure 2.7b.

For our work, we notice that both the E & H-plane the cross polar component is lower than the co-polar one by more than -20 dB. Therefore, we reached the good polarization purity and we can say that the level of the cross component is negligible.

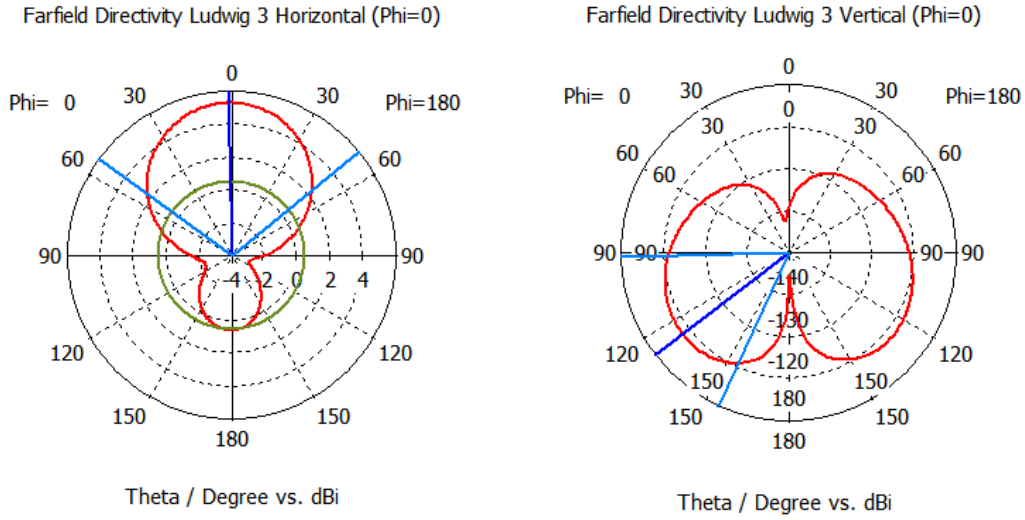

Co-polar Cross-polar

Figure 2.7a: E-plane radiation field pattern of the rectangular patch antenna at 2.45 GHz

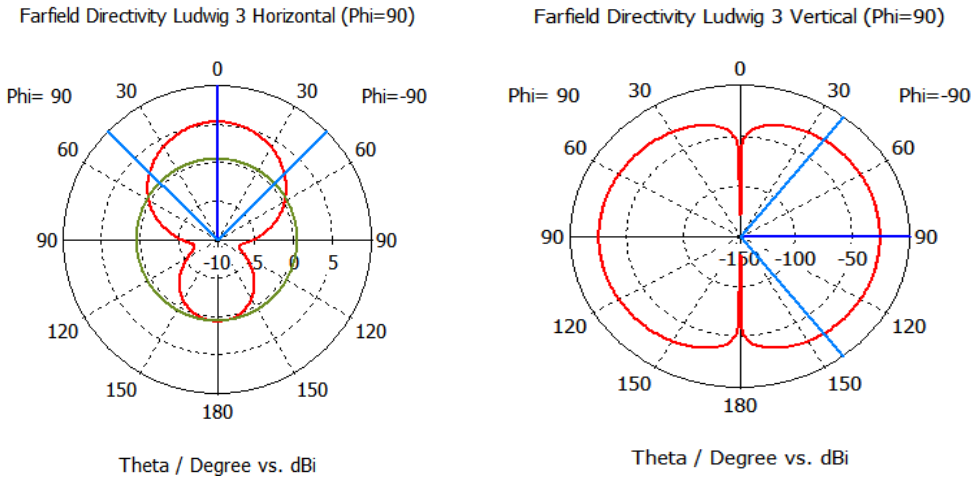

Co-polar Cross-polar

Figure 2.7b: H-plane radiation field pattern of the rectangular patch antenna at 2.45GHz

b) 3D representation of Radiation pattern.

Figure 2.8 shows the 3D representation of the radiation pattern at 2.45 GHz. It shows clearly that the rectangular microstrip antenna is a directional broadside radiating structure.

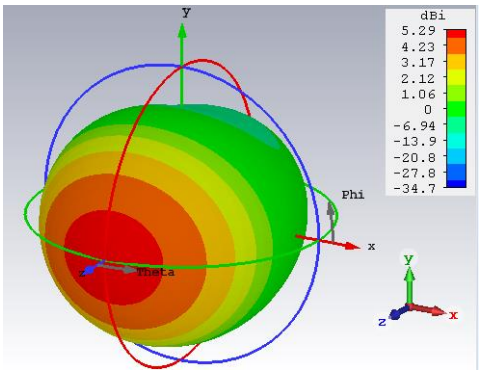

Figure 2.8: 3D view of the Radiation Pattern at 2.45 GHz

2.3 Effect of parasitic element on a rectangular microstrip antenna

This part of our work aims to study the effect of adding a parasitic element in the radiating edge of the antenna on its properties. It also intends to analyze and discuss the results. When a parasitic element is used, electromagnetic energy is coupled from the driven patch to it by the main of both the space and the surface waves, and there is a gap between any two parasitic that must be small. Here in the figure bellow, figure 2.9, we show the effect of adding a single parasitic slice to the nearest edge of the single patch seen previously. The effect of mutual coupling between the two patches is investigated.

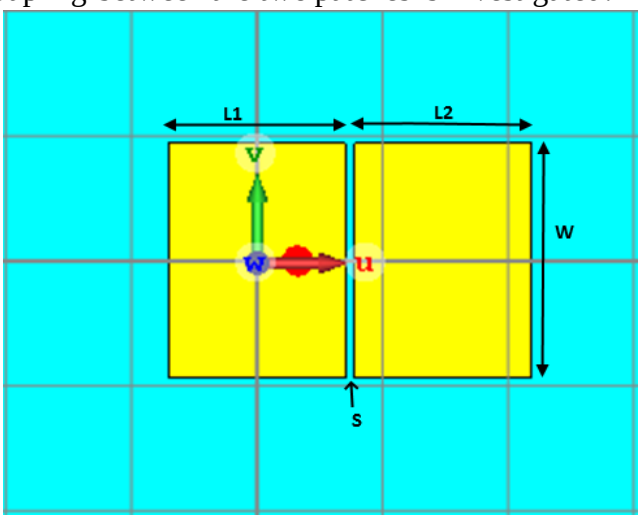

Figure 2.9: Rectangular microstrip antenna with parasitic element

Table 2.5: *Pilot and parasitic patches dimensions*

Patch length **(L1)**	Parasitic length **(L2)**	Parasitic width **(W)**	Gap Spacing **(S)**	Excitation point **(Xp)**
28.16mm	28.16 mm	37.6mm	1.5mm	(6.49,0)

As we can see in the table above 2.5, the dimensions of the parasitic patch are selected similar to those of the pilot one with letting a separation distance of 1.5mm. Knowing that the parasitic patch is added without the presentation of any other excitation point expect the one on the pilot patch at Xp = 6.49 mm.

Generally, the minimum distance between elements in an antenna array should be half of the wavelength 0.5 λ_0 for a reduced mutual coupling and better performance. However, the less the distance the better the reduction of mutual coupling. That's why it is a big challenge to bring the two antennas closer than the half while keeping mutual coupling very low. For our work, we managed to get the separation distance of 0.012 λ_0 which is very small.

2.3.1 Input reflection coefficient

The input reflection coefficient of the patch with the parasitic is shown in figure 2.10. As compared with the input reflection of the single patch (see figure 2.3) the addition of a parasitic highly affects the isolated element. The resonance frequency and the matching are both concerned by the changes done with the addition of the parasitic patch due to mutual coupling.

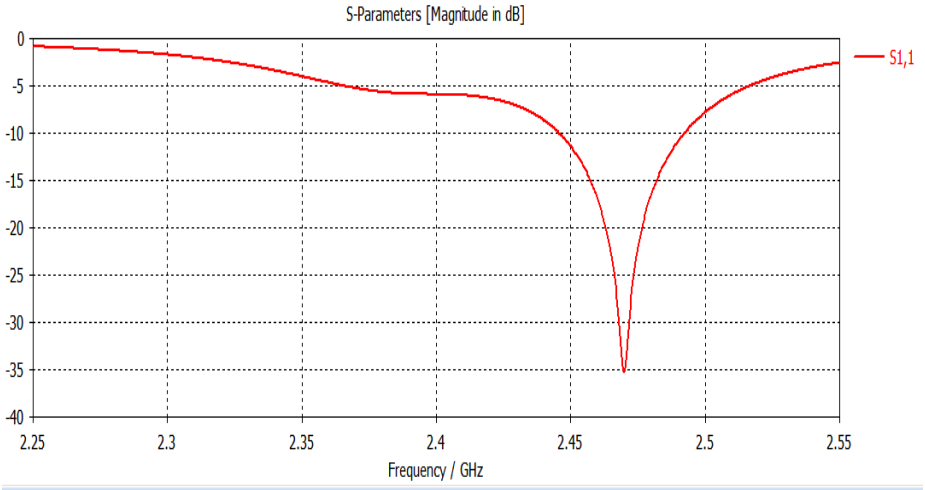

Figure 2.10: reflection coefficient of the rectangular patch antenna with parasitic element.

2.3.2 Current distribution

The current distribution at 2.45 GHz of the structure shown in the figure 2.10 is drawn in the figure 2.11. Even though the parasitic patch is not fed, some current is distributed on it indicating the effect of coupling between the two patches.

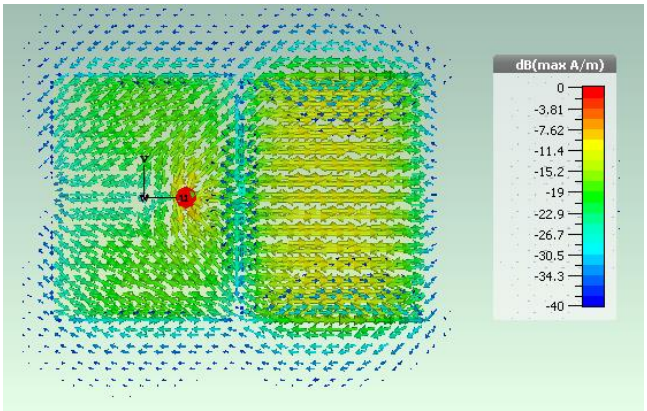

Figure 2.11: Current distribution of the rectangular patch antenna with a parasitic at 2.45 GHz

We know that it's intrinsic to the nature of antennas that when two antennas are in proximity and one is transmitting, the second will receive some of the transmitted energy, with the amount dependent on their separation and relative orientation. Even if both antennas are transmitting, they will simultaneously receive part of each other's transmitted energy. Furthermore, antennas re-scatter a portion of any incident wave and thus act like small transmitters even when they are nominally only receiving. The result is that energy interchanges between particular elements of an array. This effect is a manifestation of "mutual coupling" that exist between array antennas. It is not usually a negligible effect and complicates the design of such antennas [31]

2.3.3 Parametric study

i) The feed point position

In order to get a better matching, we have moved the feed point to X_P = -10.3 mm. The resulting input reflection graph is shown in figure 2.12.

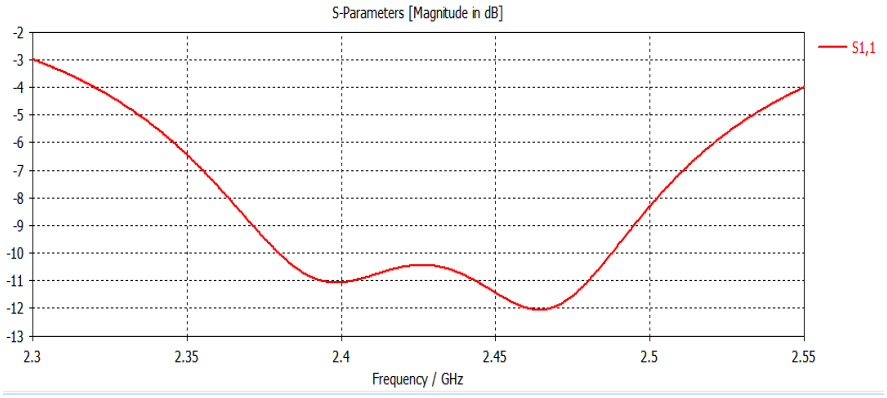

Figure 2.12: Input reflection coefficient of RMPA with parasitic element for Xp = -10.3 mm.

We can also see that the return loss at 2.4 is equal to -11 dB, the return less at 2.48 is equal to -12 dB and the bandwidth is increase equal to 6.53% when it was 2.272% for the single patch. This is explained by the superposition of the two resonances of the two patches which are closed to each other. The mutual coupling has a great impact on resonance frequency and impedance bandwidth. Owing to coupling effect we have observed that we have two resonance frequencies instead of one.

ii) Separation gap, S, effect

Mutual coupling is highly affected by the separation between the patches. In this part we will see the effect of varying the separation gap S.

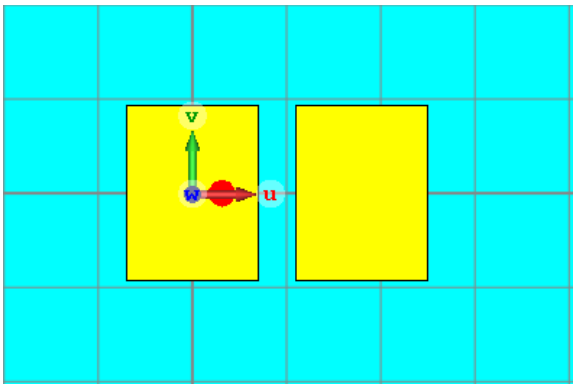

Figure 2.13: RMPA with a parasitic element for S = 8 mm

Several values of S are tried and studied in [31] so that by increasing the separation distance between patches, the mutual coupling between them are reduced. Taking S = 8mm, the mutual coupling becomes extinct. In our work, and because of the use of CST

Studio instead of IE3D, some changes have been made in order to adjust the results and obtain the good matching (see table 2.6).

Table 2.6: *Parasitic patches dimensions.*

Parasitic length**(L2)**	Parasitic width **(W)**	Gap Spacing **(S)**	Excitation point **(Xp)**
27.988 mm	37 mm	8 mm	(6.29 mm, 0)

The simulation of the structure with these values has given the input reflection coefficient and the input impedance shown in figures 2.14 and 2.15 respectively

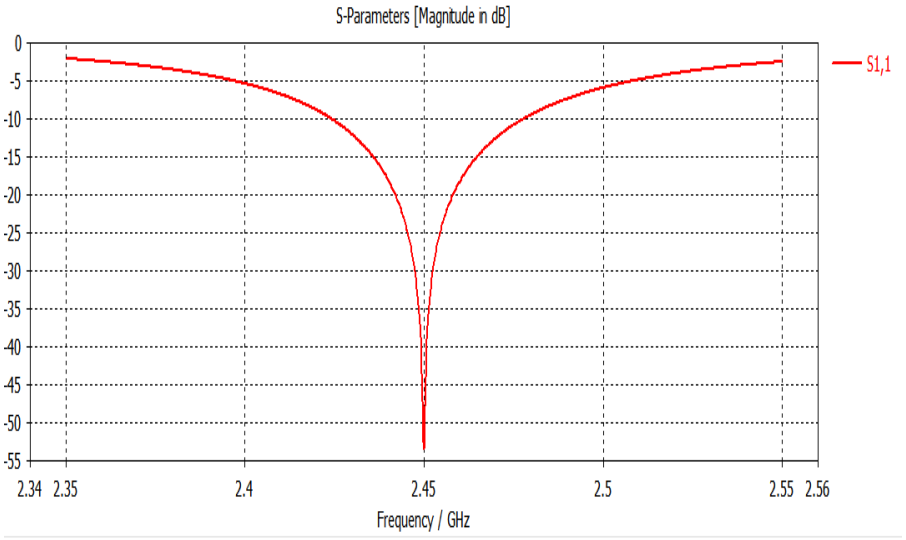

Figure 2.14: reflection coefficient for S=8mm.

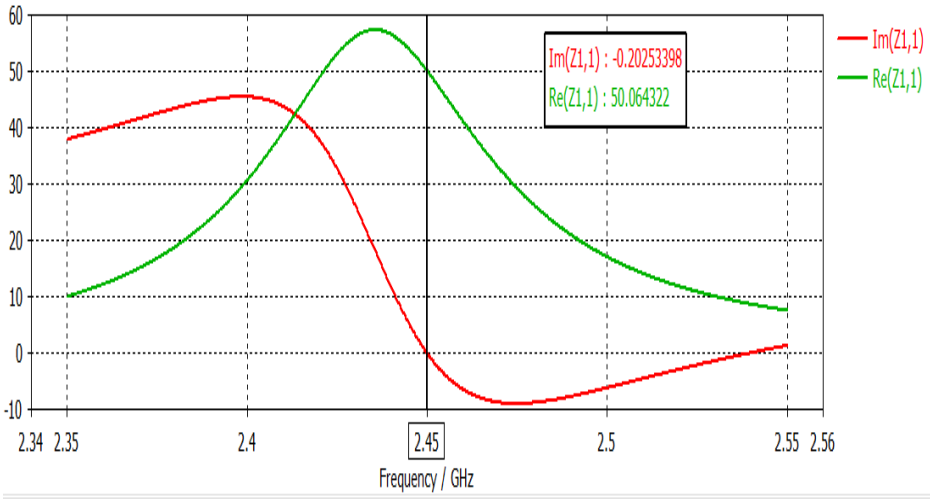

Figure 2.15: Real and Imaginary part of RMPA with parasitic element input impedance for S= 8mm

- As we can see in the figure 2.14 the second resonance frequency has been removed and best matching is realized.
- At 2.45 GHz the input impedance is 50 ohm and 0 for its real and imaginary parts, respectively as shown in figure 2.15.

Figure 2.16 illustrates the current distribution of the structures. We can see that the current in the parasitic patch is reduced as we increased the separation between the two patches and this allow as to say that the mutual coupling is also reduced.

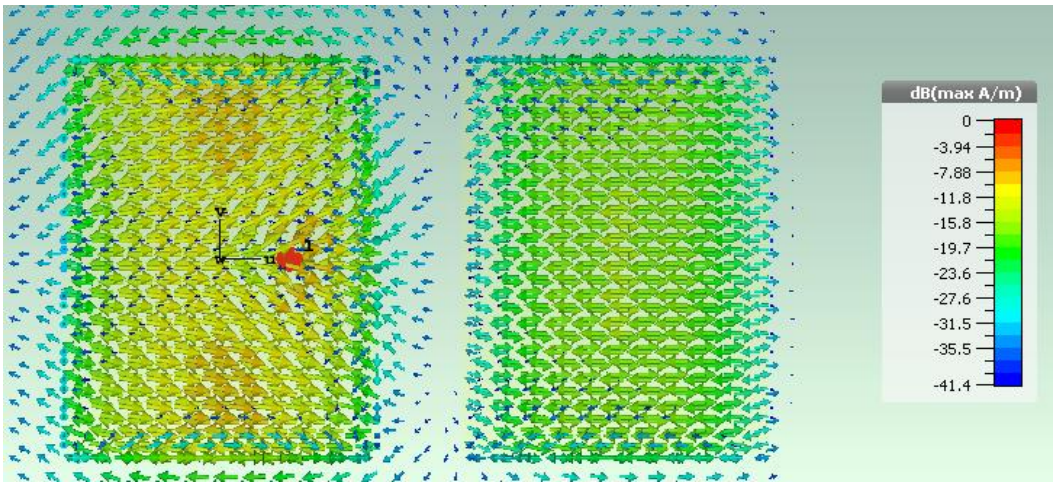

Figure 2.16: Current distribution on the two patches at 2.45 GHz for S = 8 mm.

2.4 Conclusion:

This review work describes two of the mutual coupling reduction techniques considered in microstrip patch antennas. In the first part when changing the feeding point position we got two resonance frequencies but when the gap distance S is set to 8mm we got one resonance frequency with a good matching equal to return loss of -55dB. We have seen that the mutual coupling effect cannot be definitively eliminated, but it can only be reduced.

In microstrip antennas the technique of increasing the antenna separation is mainly used.

In the next chapter, we will study another technique of reducing mutual coupling which is the effect of curvatures to the patch antenna and we will expand our study to an antenna array with four patches with and without concavity where the results will be compared. In array antennas using microstrip elements, the effect of mutual coupling should not be ignored.

Chapter 3: Linear Microstrip Array with Reduced Mutual Coupling

3.1 Introduction

In the previous chapter, we have seen that when two patches are too close to each other, the effect of mutual coupling appear leading to the variation of its input impedance and radiation pattern. It has been proved that by increasing the distance between the patches this effect may be decreased.

In this Chapter, another solution to overcome the problem of mutual coupling in microstrip array antenna will be presented. This solution is based on the use of concavity in the radiating edges of the patches and slots in the non-radiating edges without affecting the global dimensions of the structure. The studies will be extended to 4 elements antenna array with and without concavity and a comparison will be done for the best solution.

3.2 Rectangular patch and parasitic with curvatures radiating at the original frequency

In the previous chapter, we discussed a theoretical part the method used to reduce the mutual coupling effect which is the use of curvatures and slots on a rectangular microstrip patch. In this part we will show how it is done.

An elliptical curvature shape is cut from the radiating edges on the patch antenna. An ellipse is created and centered exactly on the edge of the patch; this means that only a half of the ellipse is overlapped with the patch. The ellipse is characterized with a primary axis radius (W/2) and secondary axis radius, which is called the curvature of the patch C.

Again same method is used to cut a slot in the middle of the non-radiating edges of the rectangular patch. This time, the ellipse is characterized with 6 segments points, a fixed secondary axis of 1 mm and varying primary axis that refers to as N.

The study of the effect of C and N is done in [31]. The results are as follow:

- The increase in C leads to the increase in the resonant frequency of the structure and the later is due to decrease in the resonant length of the patch leading to shortening the path of the current.

- The resonance frequency decreases as the primary axis radius N of the elliptical slots increases. This is explained by lengthening of the patch of the current as a slot is cut in the non-radiating edge.

The final structure of the two adjacent rectangular patches with curvatures and slots is presented in the figure below (figure 3.1). After several trials we recovered the original resonant frequency, the suitable slot has a width of 1 mm and depth of N = 7.6 mm. We have also fixed the following values: L = 28.943 mm, W = 29.95 mm, C = 2.9 mm, Xp = 4.88mm and S=1.5 mm (separation distance).

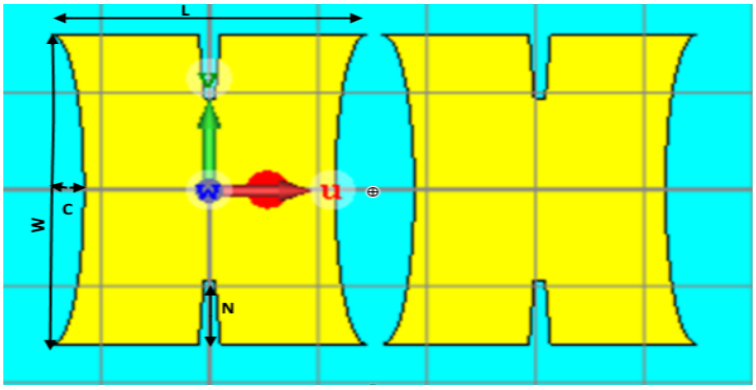

Figure3.1: Structure of two patches with curvature and slots.

3.2.1 Simulation Results

3.2.1.1 Return loss

The reflection coefficient of the structure of figure 3.1 obtained from simulation is shown in the figure 3.2. As we can see only one resonance is obtained indicating a reduction of the mutual coupling due to the used technique. Also the proper choice of the excitation point results in the very good matching; with the input reflection coefficient level about -67dB at exactly the original resonant frequency (2.45GHz).

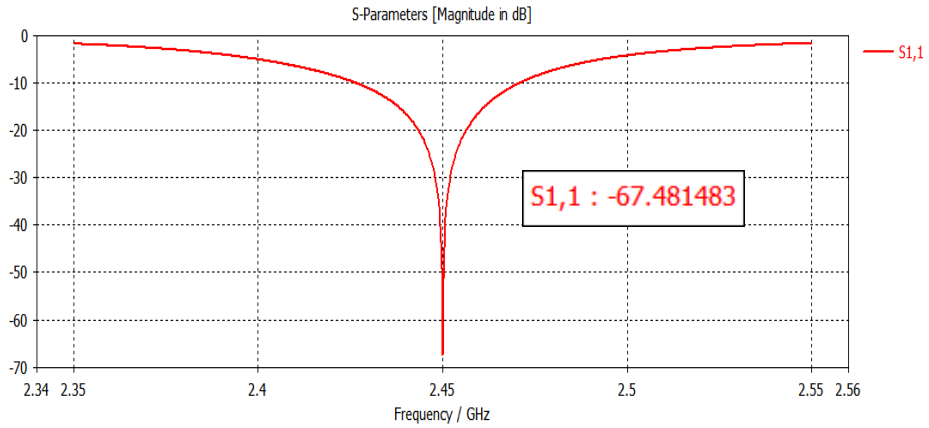

Figure 3.2: Input reflection coefficient of two patches with curvature and slots

We can also use the figure 3.2 to obtain the frequency bandwidth using the frequencies at -10dB.The calculation using (2-6)

$$BW = \frac{2.4833 - 2.4167}{2.45} \times 100 = 2.71\%.$$

Indicating that the structure has a narrow bandwidth.

3.2.1.2 Input Impedance

Figure 3.3 illustrates the input impedance of two patches with curvatures and slots. As we can see, at 2.45 GHz the impedance of the system is perfectly matched to 50 Ω.

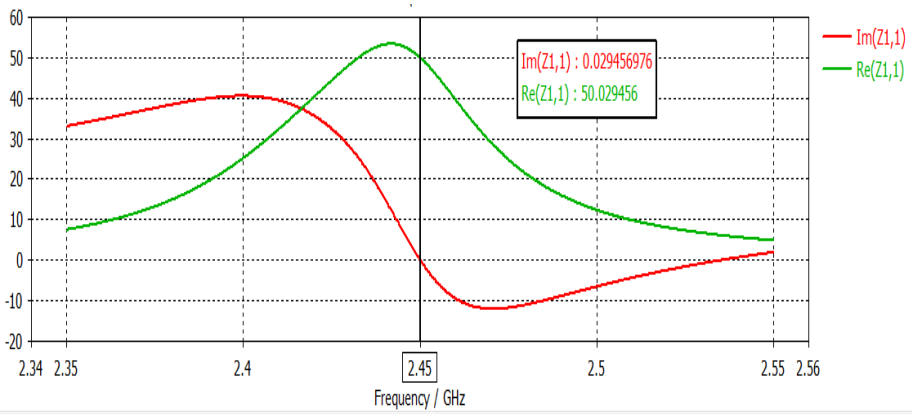

Figure 3.3: Real and Imaginary parts of the two patches with curvature and slots.

3.2.1.3 Current Distribution

To analyze the effect brought by the pilot patch on the parasitic one, the surface current distribution is shown in figure 3.4. When observing this figure, we notice that the strong current distribution mainly focuses on the pilot patch and the intensity of the current on the parasitic patch is negligible. This indicates that the use of the curvatures reduces the mutual coupling.

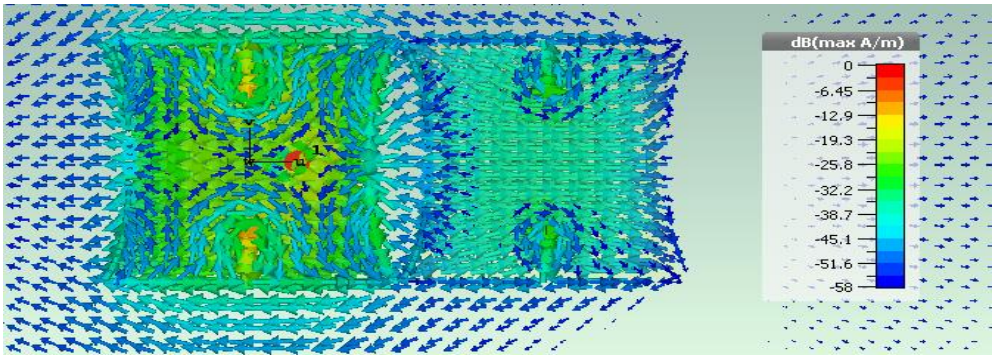

Figure 3.4: the current distribution on the two adjacent patches with reduced coupling at 2.45 GHz.

3.2.1.4 2D-Respresentation of Radiation field patterns:

The radiation pattern is presented in the polar form with the dB scale. The radiation patterns of the two adjacent patches with reduced mutual coupling operating at 2.45 GHz is drawn in the E-plane ($\phi = 0°$) => $E_{co} = E_{\theta}$ in the figure 3.5a.

The radiation pattern in the H-plane ($\phi = 90°$) is shown in figure 3.5b. In this plane, the pattern of the two adjacent patches is almost similar with the single patch pattern shown in chapter 2 (figure 2.7b) since the parasitic element is in the radiating edges and free from mutual coupling.

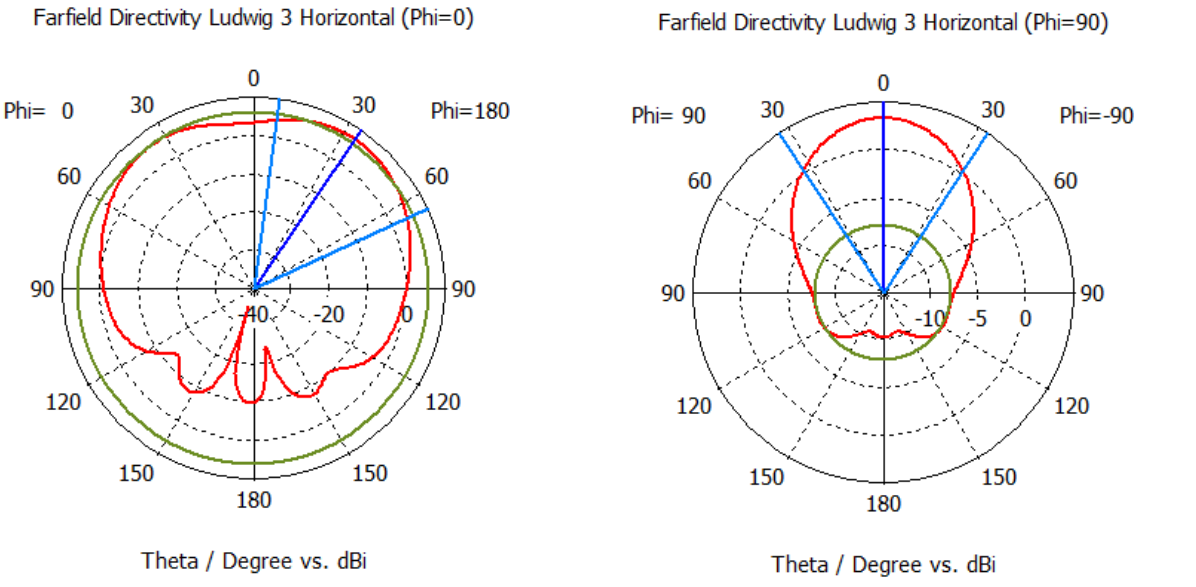

a) E-plane **b) H-plane**

Figure 3.5: E and H plane pattern for the two adjacent patches with reduced coupling at 2.45 GHz.

3.2.2 Two patches with curvature and slots compared to the one with large gap spacing:

a) Input reflection Coefficient

In order to compare the structure with concavity and slots and the one with two patches separated with large gap, we have drawn the two graphs of their input reflection coefficients. The figure 3.6 represents the two graphs obtained after the simulation of the two previously mentioned structures. We can clearly see that the one with curvatures (blue graph) has a narrower bandwidth and a better matching compared to the one with a big space gaping (red graph) with a difference of 15 dB which is due to the advantage of the curvatures when reducing the mutual coupling of our structure. However, the one with space gap is sufficient but not efficient for the case of our application.

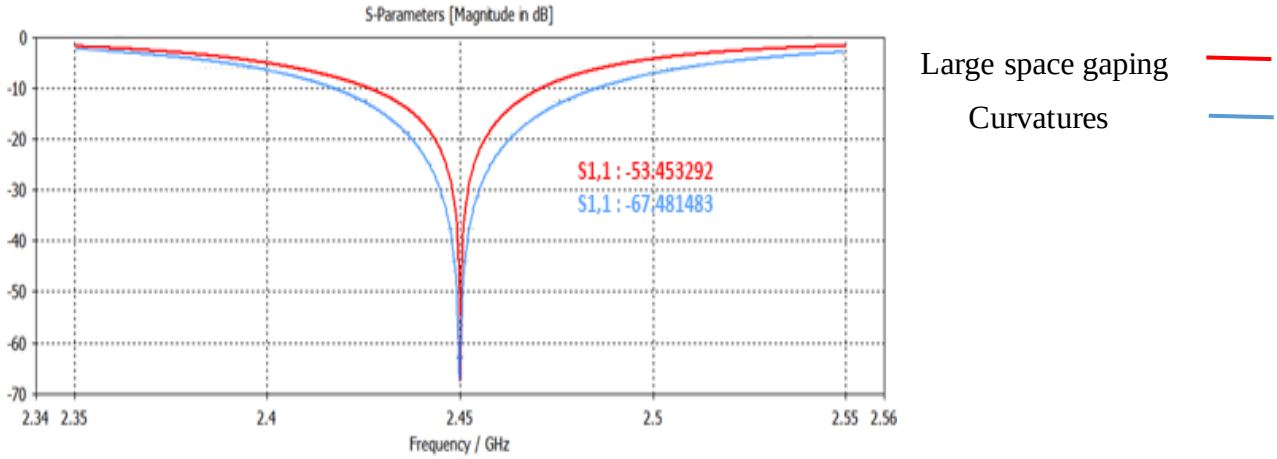

Figure 3.6: input reflection coefficient of the two structures at 2.45 GHz

b) Radiation Pattern

When it comes to far field results, we compare the results of figure 3.5 with ones of 3.7. Clearly there is not a big difference between the two, just small deviations and a difference of 2 dB, the one of 8mm space gaping is less than the one with concavity, which made it another advantage for the concavity mutual reduction technique.

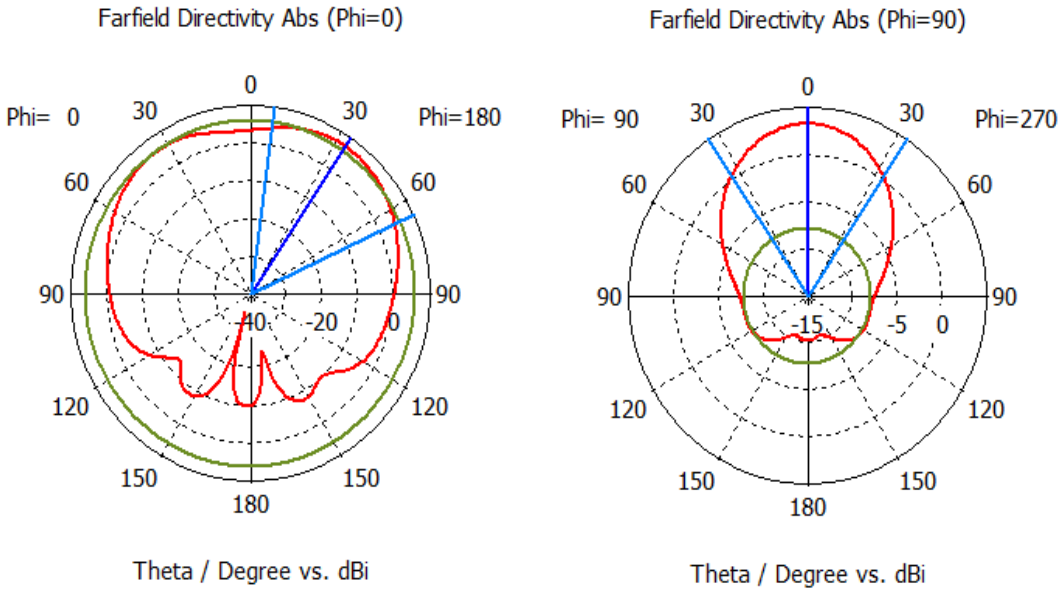

a) E-plane **b) H-plane**

Figure 3.7: E and H field radiation pattern for the two adjacent patches with S=8mm at 2.45 GHz.

3.3 Four element array antenna

Since the array procedure enhances the behavior of the microstrip patch antenna, we are going to extend our previous work to four elements array, where all the elements are fed, in order to show that the previous technique reduces mutual coupling with a

specific reduction degree.

The choice of 4 elements has been made regarding the port of the Vector Network Analyzer of our lab for eventual measurements.

3.3.1 Four element array antenna without concavity

In this part we will extend our studies done in chapter 2 to an array of four patches without concavity in order to compare it with the ones with concavity. Except that all the patches are fed at the same point and equally at the same time. The physical structure and dimensions of the proposed 4-element antennas are shown in figure 3.8 and table 3.1 respectively. The array elements are identical and are separated by same gap distance.

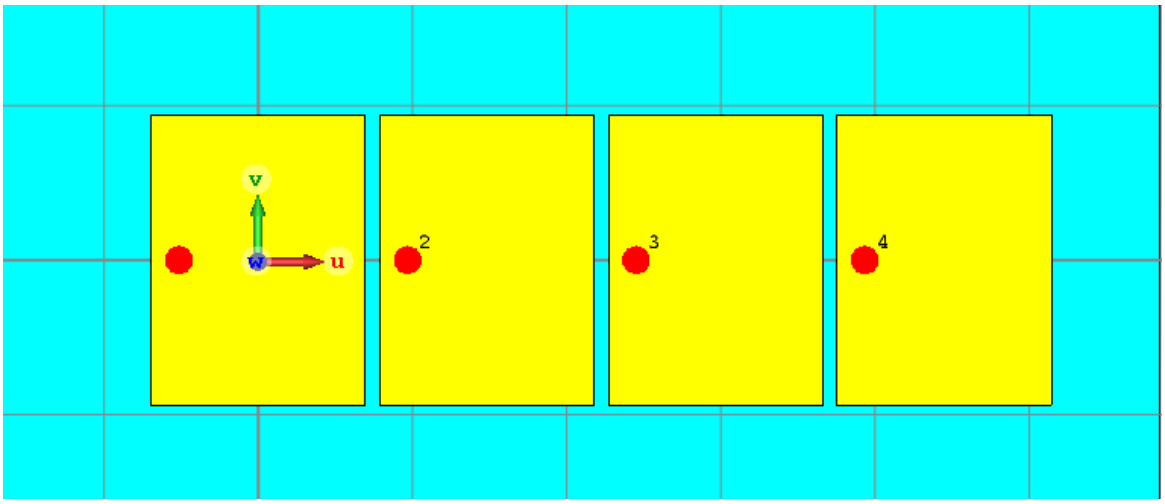

Figure 3.8: 4-element normal rectangular microstrip array antenna at 2.45 GHz.

Table 3.1: *Dimensions of the rectangular patch used in the array*

Length	Width	Excitation point	Gap spacing
L=28.16 mm	W= 37.6 mm	Xp=(-10.3,0)	S=1.5mm

In the previous sections, the exsitance of the mutual effect between microstrip patches, in a structure containing more than one patch, is verified only qualitatively via the input reflection coefficient and the current distribution. Here, this effect will be quantified by finding the transfer coefficient, S_{ij}, between different patches.

After simulating the structure, the obtained results are graphically shown in figure 3.9. This figure indicates clearly that the patches interact between each other since the lowest level (S_{14}), at the resonant frequency, shown in the figure is only –18 dB and occurs between the far elements, the first and the fourth. The close elements are strongly coupled with a level around -8 dB.

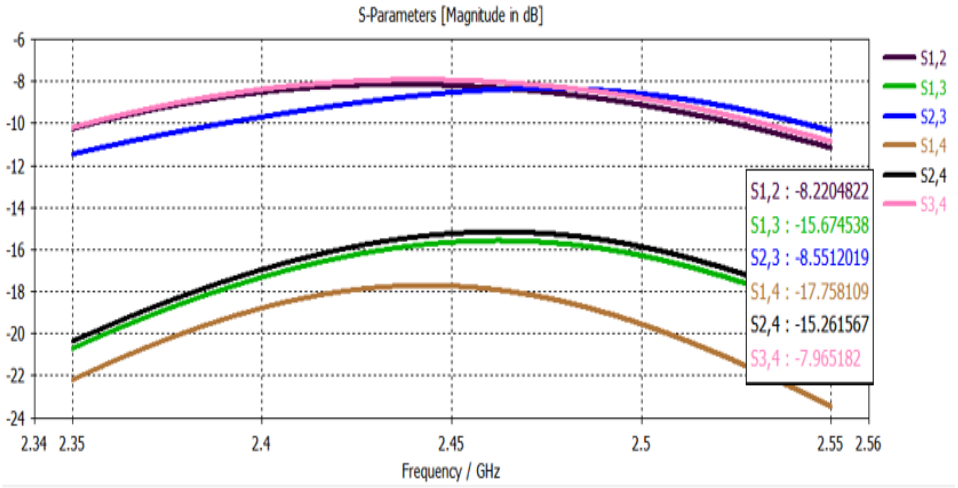

Figure3.9: Coupling coefficients of the 4-element normal rectangular patch array antenna.

Figure 3.10 shows the 2-D polar plot of the E plane and H plane field radiation pattern for the microstrip patch antenna array. The radiation pattern of the array is evaluated as the sum of the contribution of each element. The element pattern, however, is influenced by the presence of the neighbors and is different from the one of the isolated element.

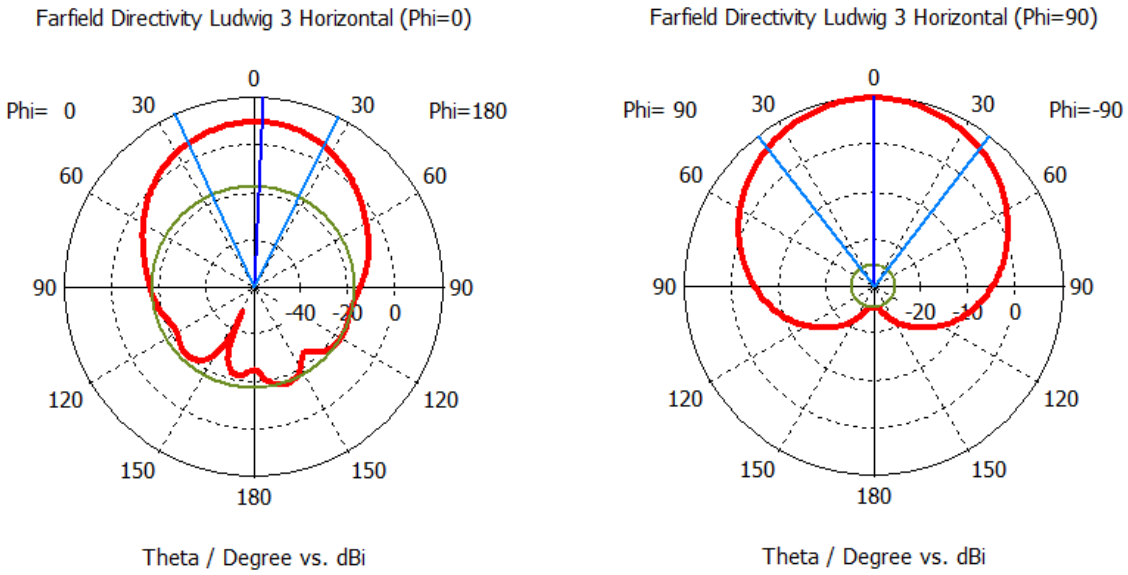

a) E-plane **b) H-plane**

Figure 3.10: E-plane and H-plane radiation pattern for the normal rectangular array.

3.3.2 Four element array antenna with concavity

When it comes to this part of our work, we have extended the studies done in the first part of this chapter to 4 elements, by keeping the same feeding point (Xp = 4.88 mm) position and applying it on the 3 others as shown in figure 3.11. The purpose of this operation is to study the network of the microstrip patch antenna array with the previous reduced mutual coupling results to see the effect on its S-parameters. S=1.5 mm

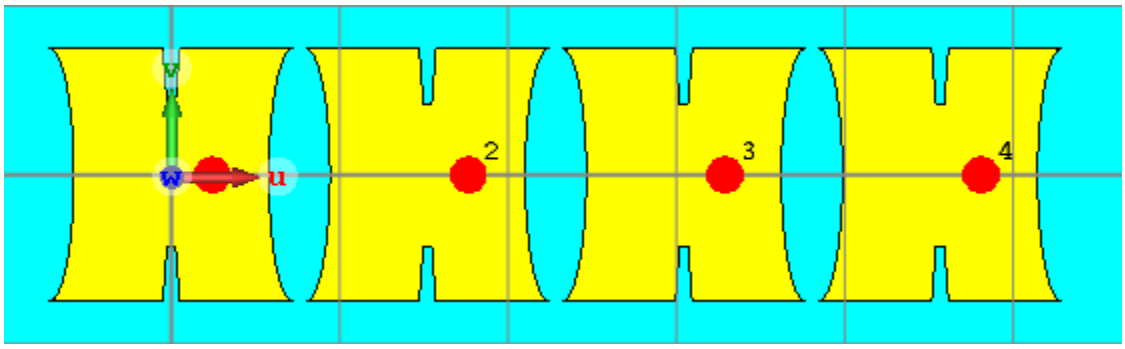

Figure 3.11: 4-element rectangular patch array antenna with concavity and slots.

3.3.2.1 Simulation results

- **Input Reflection Coefficient**

After the simulation of the previous antenna, using the CST software we were able to get the following results.

Figure 3.12 represents the return loss parameters of our array, it is clear that all the ports are matched at the operating frequency below -10 dB.

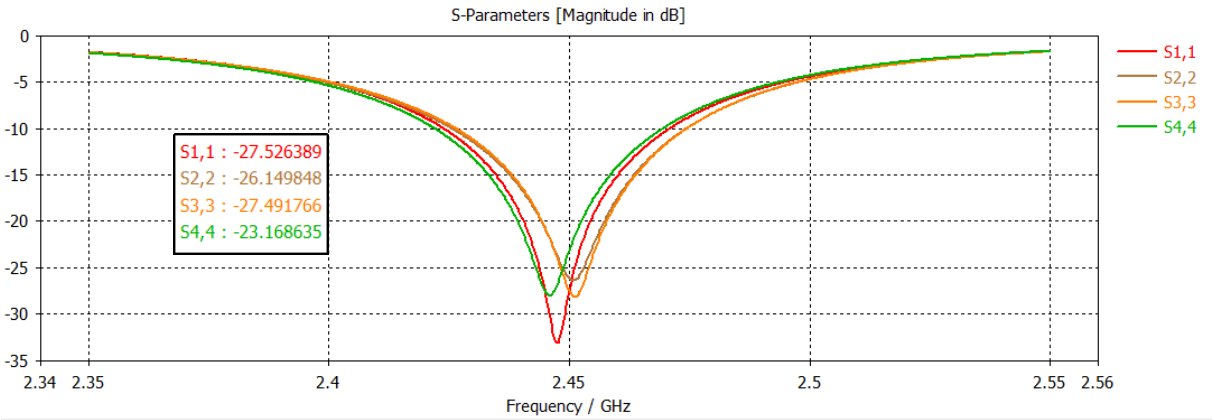

Figure 3.12: Input Reflection Coefficients S_{11}, S_{22}, S_{33}, S_{44} of the four elements of the rectangular array antenna with concavity at 2.45 GHz

Figure 3.13 illustrates the transfer parameters between the elements of the rectangular array with concavity. As compared to the case of the array with normal rectangular elements, the level of the transfer parameters is reduced by an average value

-7 dB because of the concavity introduced in the radiating edges of the rectangular patches. The parameters between the closest elements are passed from -8dB to -15 dB and those of the far elements are passed from -18 dB to -23 dB.

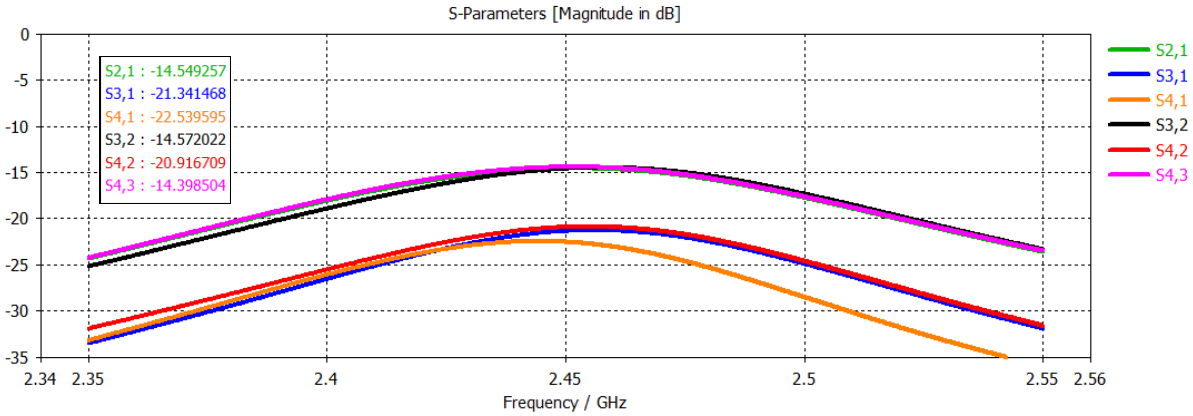

Figure 3.13: Coupling coefficients of the 4-element rectangular patch array with concavity

- **Radiation Pattern**

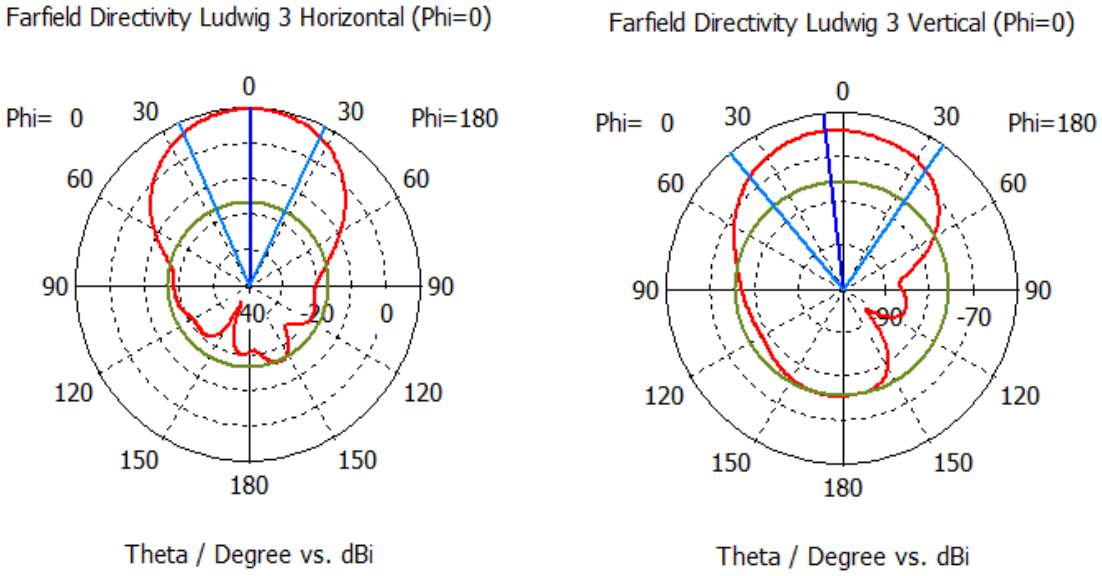

(a) Co-polar **(b)** Cross-polar

Figure 3.14a: E-plane, co & cross polar components radiation field pattern of 4 elements microstrip patch antenna array at 2.45 GHz.

From Figure 3.14 (a) & (b) we can notice that the cross-polar component is lower than the one of the co-polar, which can lead to a good polarization purity.

We mainly notice the maximum value in the co-polar component at both E & H plane due to the excitation amplitude controlled by the CST software.

We also can see some deviation on the back lobes and the small level of side lobes on both planes.

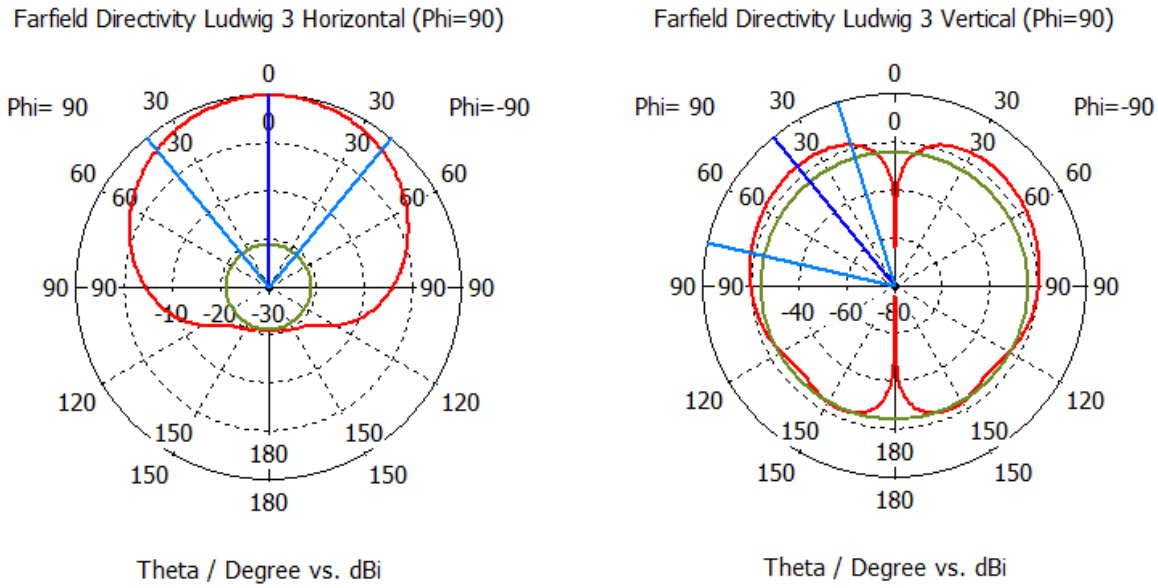

(a) Co-polar **(b)** Cross-polar

Figure 3.14b: H-plane, co & cross polar components radiation field pattern of 4 elements microstrip patch antenna array at 2.45 GHz.

3.3.3 Comparison between array with and without concavity.

For the application of any antenna array, the reduction of mutual coupling is a must for a good performance of the network. It can be seen by a simple comparison between the coupling coefficients of both our linear four elements microstrip antenna array with and without concavity.

After analyzing our results, figure 3.9 and figure 3.13. We can notice that coupling coefficient of the optimal concave array in the resonant frequency is good, about 7 dB less than the one of the ordinary rectangular array antenna, representing the mutual coupling reduction degree. Overall, the proposed optimal concave array antenna has low amounts of mutual coupling with a 7 dB degree.

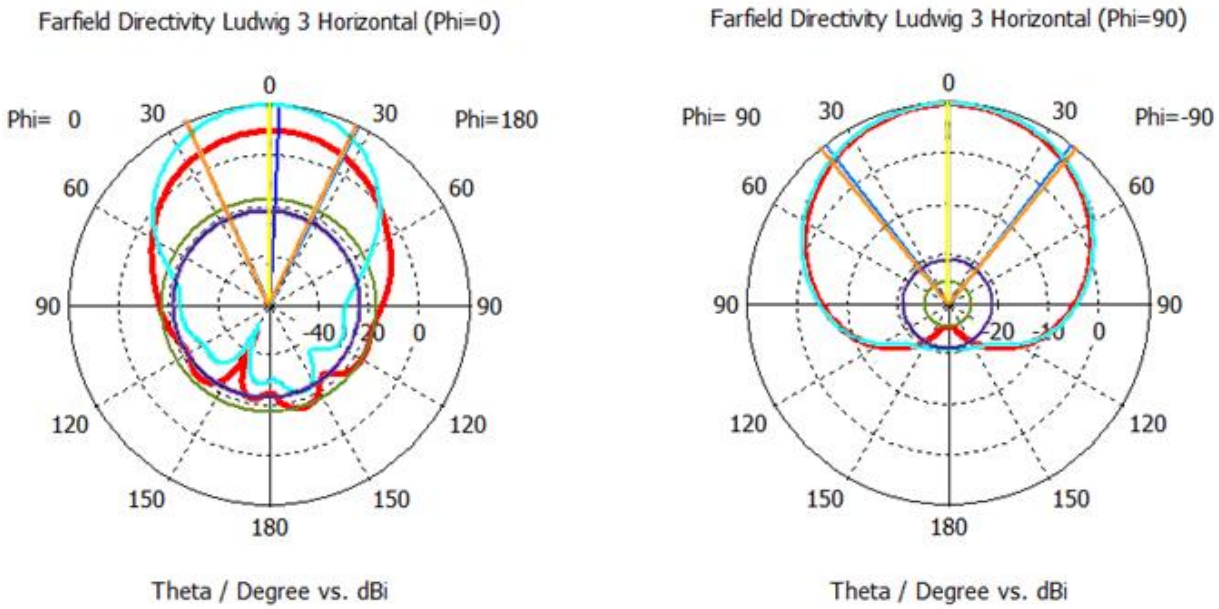

Figure 3.15: E and H-plane radiation field pattern of 4 elements microstrip patch antenna array with and without reduced mutual coupling at 2.45 GHz.

Represents the pattern of our array with reduced mutual coupling.

Represents the pattern of our array without reduced mutual coupling.

The simulation results, Figure 3.15 shows a clear improvement in the directivity and the gain, at both planes. The shape of our patterns didn't change much, Some small deviation has been observed for the case of the array without reduced mutual coupling at the H-plane and a shift of 3° toward the maximum for the case of the array with reduced mutual coupling in the E-plane. Explained by the fact that the mutual coupling effect affects the radiation pattern by the cancelation effect resulted from the induced and the main radiations.

Another element that should be mentioned is the half power (-3dB) beamwidth in the maximum radiation direction at the operating frequency of our application, 2.45 GHz.

Table 3.2 summarizes the radiation characteristics and propagation information extracted from the radiation pattern for all the structures that have been studied before.

An amelioration of a 4.36 dBi directivity from the single patch to the final 4 elements array with concavity is presented along with the -3dB beamwidth at the maximum radiation.

Table 3.2: *Antenna's radiation characteristics at 2.45 GHz.*

Structure	Beamwidth (°)	Maximum Direction of propagation(°)	Maximum Directivity (dB)
Single patch	E-plane 104.8°	1°	5.29 dBi
	H-plane 90.4°	0°	
2 patches with large space gaping.	E-plane 57.5 °	34°	7.17 dBi
	H-plane 66.7°	0°	
2 patches with concavity.	E-plane 48.2°	38°	8.21 dBi
	H-plane 85.5 °	0°	
4 elements antenna array without concavity.	E-plane 90.4°	3°	9.62 dBi
	H-plane 75.4°	0°	
4 elements antenna array with concavity.	E-plane 50.0 °	1°	9.65 dBi
	H-plane 78.7°	0°	

3.4 Design of a 1-to-4 Wilkinson Power Divider for antenna array feeding network

In perspective of realization and measurement of the designed arrays, the Wilkinson power divider appears more appropriate and it can easily be used to feed the array based on the coaxial feeding. So, in this section a 1-to-4 Wilkinson Power Divider is designed.

3.4.1 Parameters to be considered while designing a Wilkinson Power Divider

As mentioned in the first chapter, Wilkinson power divider is the best choice for feeding an antenna array network for its possibility of meeting the ideal network conditions (if it is matched at all ports) being lossless, reciprocal, matched. However, the following parameters are to consider while designing a power divider. The parameters are [35]

- Insertion loss
- Return loss
- Isolation loss
- Bandwidth
- Input and output Impedance

3.4.1.1 Insertion Loss

Insertion loss is the loss of signal power resulting from the insertion of a device in a transmission line or optical fiber and is usually expressed in decibels (dB). The ideal value of insertion loss is 0 dB. The insertion loss is defined as

$$\text{The Insertion loss (dB)} = 10 \log (P_i/P_o)$$

Where P_i: Maximum amount of power that can be transmitted before the insertion of a device in a transmission line.

P_o: Maximum amount of power that can be received after the insertion of a device in a transmission.

3.4.1.2 Return Loss

Return loss or reflection loss is the loss of signal power resulting from the reflection caused at a discontinuity in a transmission line or optical fiber. This Discontinuity can be a mismatch with the terminating load or with a device inserted in the line. It is usually expressed in decibels as given in Equation (2.3).

3.4.1.3 Isolation Loss

Isolation is the insertion loss in the open path of a switch or between two ports on a passive device. It is measured between any one of the output port and input port with the condition of another port in terminating condition. It allows the signal only in the forward direction value should be high. The Isolation loss is defined as

$$\text{Isolation loss (dB)} = 10 \log (P_o/P_i)$$

Where, P_o: Amount of power received at output ports.

P_i: Amount of power incident on a transmission line.

3.4.1.4 Bandwidth

The 10 dB bandwidth is commonly calculated for return loss where VSWR is less than 2 and more than 90% of signal transmitted as shown in equation 2.6.

3.4.1.5 Input and Output Impedance

The design of microstrip power divider is constructed using one input and 4 output ports which are terminated by 50 ohm. The characteristics impedance of microstrip line and

microstrip curved bend are 50 ohm and 70.71 ohm as shown in the table 3.3 and figure3.16.

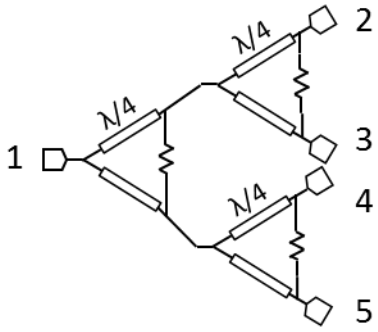

Figure 3.16: Block Diagram, of a 4 output ports Wilkinson power divider

Table 3.3: *Ideal design parameters of Wilkinson power divider*

Z0	2Z0 (shunt resistor)	$\sqrt{2}$ *Z0* (characteristic impedance)
50 Ω	100 Ω	70.71 Ω

3.4.2 Dimensions of microstrip lines

In our work, the design of the Wilkinson power divider is done in microstrip lines of 50 ohm and 70.71 ohm and the initial dimensional expression is to be calculated by using equation (3.1) to (3.5) programmed in MATLAB environment. [36]

- The effective dielectric constant of a microstrip line:

$$\varepsilon_{eff} = \frac{\varepsilon_r+1}{2} + \frac{\varepsilon_r-1}{2}\left[\frac{1}{\sqrt{1+12(\frac{w}{d})}}\right] \quad (3.1)$$

For given characteristic impedance Z_0 and dielectric constant $\boldsymbol{\varepsilon_r}$ the $\frac{w}{d}$ ratio can be found as:

$$\frac{W}{d} = \frac{8e^A}{e^{2A}-2} \quad (3.2)$$

Where

$$A = \frac{Z0}{60}\sqrt{\frac{\varepsilon_r}{2}} + \frac{\varepsilon_r-1}{\varepsilon_r+1}\left(0.23 + \frac{0.1}{\varepsilon_r}\right) \quad (3.3)$$

$\boldsymbol{W}$ is the width of the microstrip line and $\boldsymbol{d}$ is the substrate thickness.

The length of the microstrip line *l* and the velocity factor K_0 are related to the operating frequency f_0 with a phase shift of 90° as

$$K_0 = \frac{2*f_0*pi}{c} \tag{3.4}$$

$$l = \frac{90*(pi/180)}{K_0*\sqrt{\varepsilon_{eff}}} \tag{3.5}$$

The calculations using the previous formulas result in the values given in table 3.4

Table 3.4: *Dimensions of the microstrip line for different impedances and at 2.45 GHz*

Impedances (ohm)	Width (mm)	Length (mm)
50	3.1118	16.9
70.71	1.6549	17.3
100	0.7288	17.8

3.4.3 Design Procedure

To feed our network, the power divider must operate at the same operating frequency, 2.45 GHz, and using the same substrate material as our array (FR4 glass epoxy) to achieve the matching for all the five ports. For our case it is required to have an equal power for the output ports and a good isolation between them.

3.4.3.1 Dimensions adjustments for 50 ohm line impedance

The power divider network is implemented in the software environment as shown in figure 3.17. Since there is a slight difference between the theory and the simulation, we had to make some changes in the calculated dimensions to reach the 50 ohm line impedance at the five (5) ports. Where it is lower than 50 we had to make it narrower and if it is too high we made it wider. Then, we terminated our ports with a waveguide port, which 50 ohm by default in the software used CST MWS.

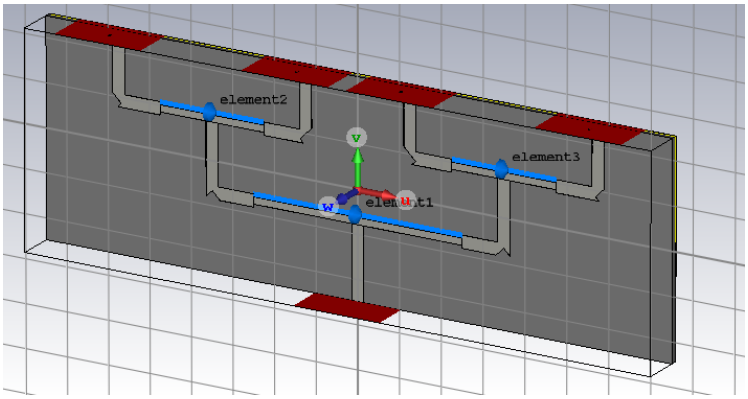

Figure 3.17: 3D view of the Wilkinson power Divider showing the waveguide ports.

After assigning the ports and adjusting the width and length of the microstrip line, and after many attempts and variation of the microstrip sharp bends and the other dimensions we were able to find the final dimensions that are presented in the table 3.5 & 3.6 and shown in figures 3.18 & 3.19.

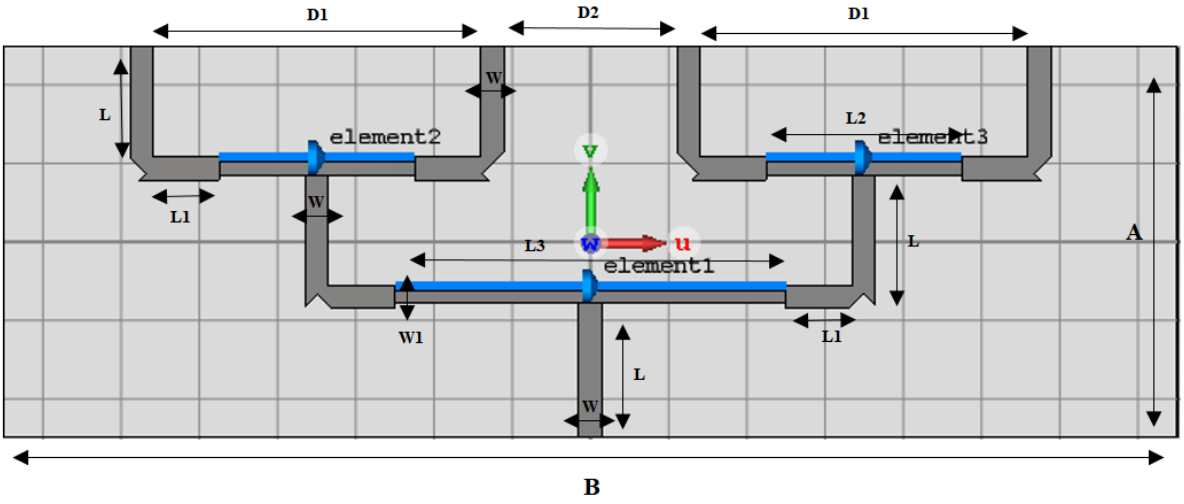

Figure 3.18: A Wilkinson Power Divider with optimized dimensions

Table 3.5: *The ground dimensions and the distance between the output ports*

A	B	D_1	D_2
49.67 mm	150 mm	33.5 mm	25 mm

Table 3.6: *Width & Length of the microstip line at 50 ohm and 70.71 ohm*

L	W	L_2	W_1	$L_1 = (L/2)$	L_3
17 mm	2.93 mm	25 mm	1.6 mm	8.5 mm	50 mm

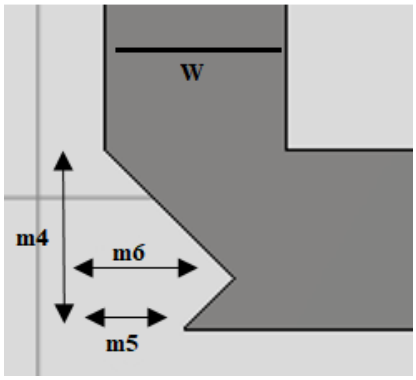

(a). Dimensions of the bend at port 2 and 4

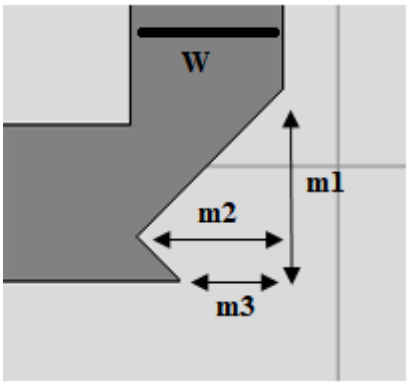

(b). Dimensions of the bend at port 3 and 5

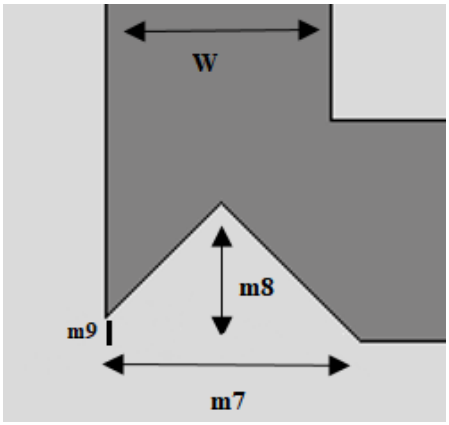

(c). Dimensions of the right and left sharp bends of the input port (1)

Figure 3.19: The dimensions of the bend at the 5 ports.

The final demensions results of the different sharp bends that suits our work are summarized in the table 3.7.

Table 3.7: *Dimensions of the sharp bend at the 5 ports of the power divider*

m_1	m_2	m_3	m_4	m_5	m_6	m_7	m_8	m_9
2.93mm	2.1mm	1.27mm	3.63mm	1.97mm	2.8mm	3.3362mm	1.8362mm	0.3362mm

3.4.3.2 Simulations Results

a) Return Loss

The input and output return loss are represented in picture 3.20. It shows that all the graph are better than -10 dB at the operating frequency 2.45 GHz leading to a good matching for all the ports and especially at the input impedance as it is -24.72 dB

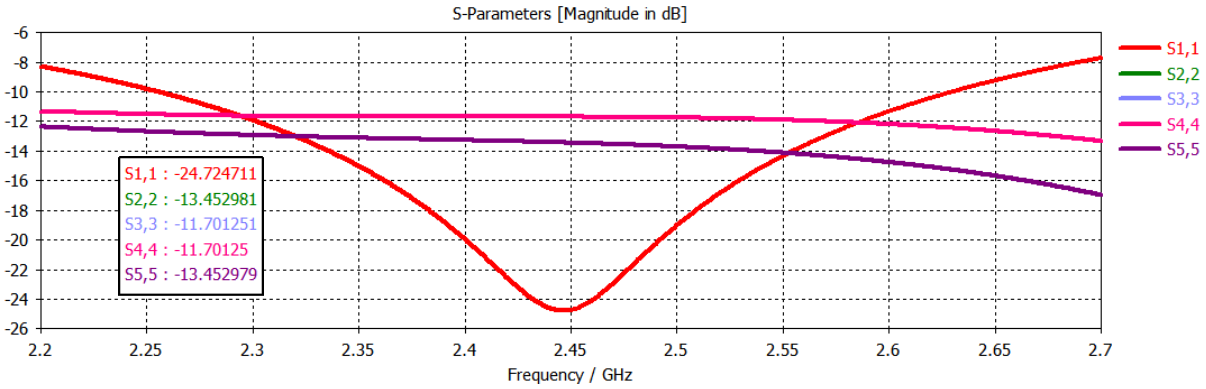

Figure 3.20: 1:4 Wilkinson Power Divider S_{11}, S_{22}, S_{33}, S_{44}, S_{55} Return loss at 2.45GHz.

b) Insertion loss

Figure 3.21 shows that S_{21}, S_{31}, S_{41}, S_{51} are almost identical $S_{21} = S_{31} = S_{41} = S_{51}$ explained by the fact that input power is equally divided between its output ports; showing a satisfactory performance with minimum insertion loss, 6.89 dB at 2.45 GHz.

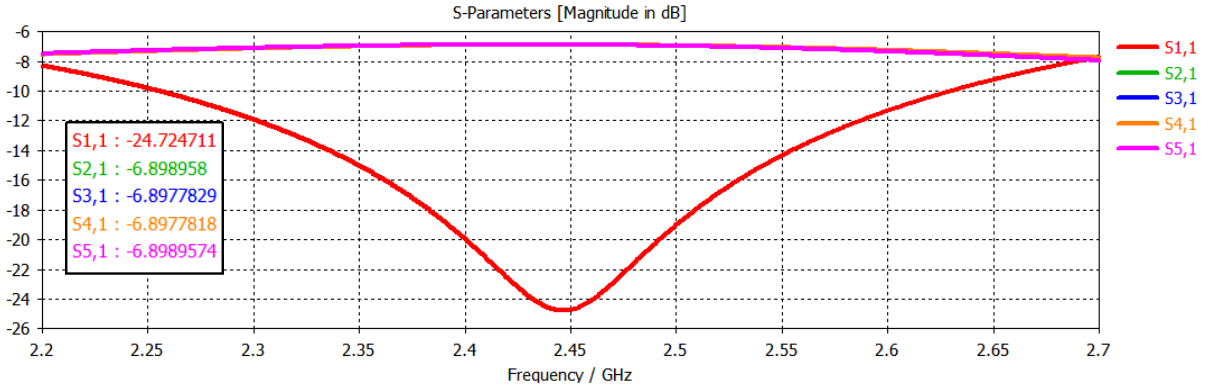

Figure 3.21: 1:4 Wilkinson Power Divider S_{11}, S_{21}, S_{31}, S_{41}, S_{51} Insertion loss at 2.45GHz.

c) Isolation

As part of the simulation results, we have obtained the graphs represented in figure 3.22. Showing that:

- The power divider is reciprocal (S_{ij}=S_{ji}).
- $S_{42} = S_{24} = S_{53} = S_{35} = S_{52} = S_{25} = S_{34} = S_{43} \backsim$ -13.49 dB => are identical, Good isolation.
- $S_{32} = S_{23} = S_{45} = S_{54}$ = - 4.85 dB => insufficient isolation.

The unsatisfactory isolation between port 2&3 and 4&5 is due to the distance between the ports. However, for our work, this is widely enough to be incorporated into our array network.

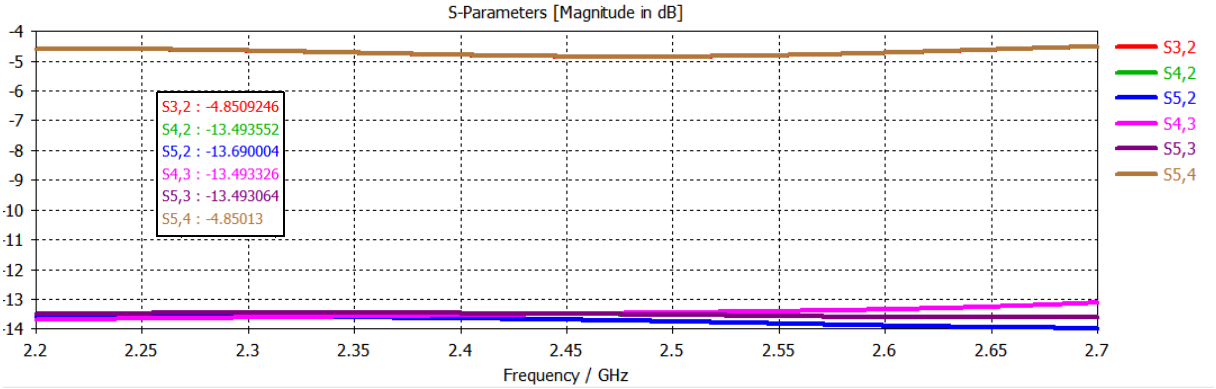

Figure 3.22: 1:4 Modified Wilkinson Power Divider S_{32}, S_{42}, S_{52}, S_{23}, S_{43}, S_{53}, S_{24}, S_{34}, S_{54}, S_{25}, S_{35} Isolation at 2.45 GHz.

d) Voltage Standing Wave Ratio (VSWR)

The figure 3.23 represents the 5 VSWRS of the 5 ports, respectively. Where all the graphs are below 2 along the range 2.2-2.7 GHz except the one of the input port that start approximately from 2.25 to 2.63 GHz, explaining a narrower band.

However, at the exact operating frequency 2.45 GHz, we can see that all that values of the VSWR are below 2. This leads to the good performance of our Wilkinson Power Divider at 2.45 GHz.

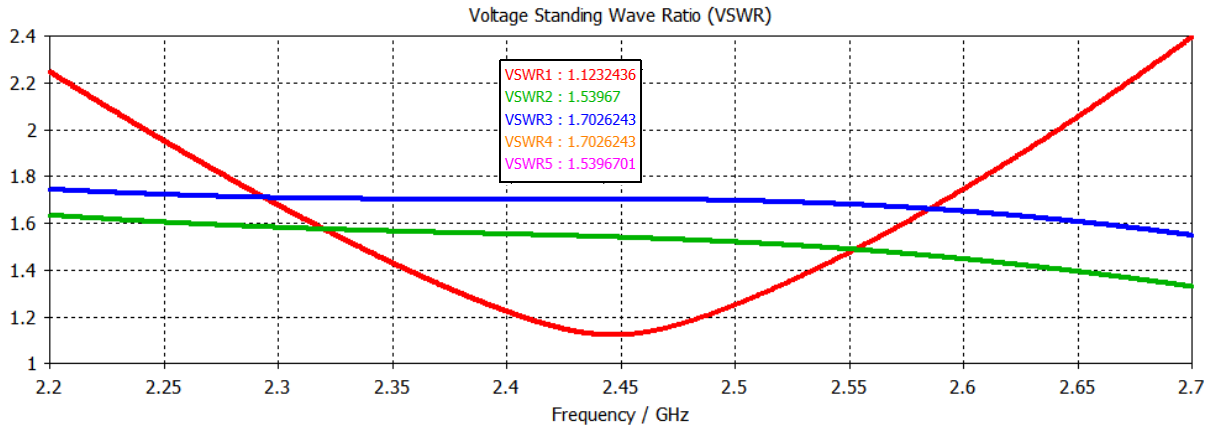

Figure 3.23: Voltage Standing Wave Ratio of 1:4 Wilkinson Power Divider at 2.45 GHz.

3.5 Conclusion:

This chapter of our work demonstrates the second method studied to reduce the effect of mutual coupling and are extended to a four (4) elements microstrip antenna array application which is required for the next generation of mobile communication (5G).The new dimensions 28.943 mm x 29.95 mm of our new shaped antenna has be developed from the chapter's two rectangular antenna. The simulation results and the comparison done with the technique explained in the previous chapter, 8 mm space gaping between the two antenna elements, have proved that a patch with concavity on the radiating edges and slots on the non-radiating with an identical parasitic at 1.5 mm distance give a better matching, gain and directivity at 2.45 GHz.

To enhance the advantage of using the concavity technique to eliminate the mutual coupling, we extended our work to 4 elements linear array, where it is the mostly used due to the importance of small distance spacing especially for beamforming and future generation communication systems. The Return loss and radiation patterns of our array were studied and discussed and a comparison between the two (2) arrays with and without concavity has been made. Hence, from the results, it is clear that the array with concavity has nearly eliminate all the mutual coupling and gave a good matching for our network.

Finally, to feed our array we designed a 1:4 Wilkinson power divider, with 4 matched ports. The Simulation showed a good isolation, insertion and return loss results. For any eventual measurements, we will feed our antennas equally at the same time using the 4 ports of our Network Analyzer and another time its one port with the input port for the power divider.

General Conclusion

In order to design a perfect array microstrip antenna, it is necessary to achieve a high gain due to the high path loss at mm-wave frequencies and reduce the mutual coupling effect. The presented work dealt with the analysis, design and simulation of 4 elements Linear Microstip Antenna array using transmission line model, excited using a coaxial probe feed with reduced mutual coupling and a wilkinson power divider to feed the network. The proposed structure operates at 2.45 GHz, modeling and performance evaluation of the proposed antennas have been carried out using the **CST Microwave studio**.

Numerical studies were first conducted for the pilot, design and simulation are done and results in a **37.6 x 28.16 x 1.6 mm** rectangular patch with a reflection coefficient of -55 dB and extended to 2x1 linear array. A non-exited patch with the exact same parameters is placed in a close distance to the excited patch lead to a high level of mutual coupling that must be eliminated.

Furthermore, two solution to reduce the mutual coupling has been presented and proved that one is more efficient than the other: The use of curvatures in the radiating edges and slots in the non-radiating edges with dimensions of **29.95 x 28.943 x 1.6 mm** with **N= 7.6mm** and **C =2.9 mm** and the enlargement of the separation distance between the patches with S=8mm. It is evident from the results that the one with concavity reduces the mutual coupling more compared to the big space gaping. Where the first one has a narrower bandwidth and a better matching compared to the second technique with a difference of 15 dB in term of return loss, which is due to the advantage of the curvatures. When it comes to the radiation pattern, it's demonstrated that there is a difference in gain of 2dB, making it another advantage of using curvatures in addition to the small space occupation which is required in the application of our 4 elements array.

The four (4) elements of our array are all excited, in both cases: concavity and without suing simple patch (pilot).Where the separation distance between element is set to be 1.5 mm, which is very small as compared to the operating wavelength and the global dimensions of the patches. The level of the transfer parameters in the array with concavity is reduced. The parameters between the closest elements are passed from -8dB to -15 dB

and those of the far elements are passed from -18 dB to -23 dB, which is due to the concavity on the radiating edges. The shape of our radiation pattern didn't change much and an amelioration of a 4.36 dBi directivity from the single patch to the final 4 elements array with concavity is presented. Overall, the proposed 4x1 array antenna with concavity has high gain with good impedance matching and a good performance in terms of 3dB beamwidth, gain, directivity and coupling parameters (S-parameters). The last shows a low amounts of mutual coupling with a 7 dB degree.

To investigate the feasibility, test our linear array and develop this project, an eventual implementation is to be done in the future and for that purpose a Wilkinson power divider with 4 outputs ports is designed and simulated using the same dielectric substrate and operating at the same frequency as the antennas. The input and output ports are all matched with an input reflection coefficient of -24.72 dB leading to a good performance and the equal division of the input power.

Many different experiments and implementations can be added in the future since it was not possible to fulfill all the requirements of this challenging work due to the lack of time and equipment in the actual situation. It proposed:

- Study of concavity effect along the non-radiating edges in planar microstrip patch antenna arrays, 8, 16, 32… elements with a corporate feed.
- Increase in the frequency to SHF and EHF bands.
- Generalization of this technique to two-dimensional configuration.

References

[1] Koushal Singh Mourya &Gaurav Chaitanya, « Advancement of Various Types of Array Structures for Smart Antennas» IEEE Indian Antenna Week 2015, At Ajmer India.

[2] Mir Riyaz Ali « Design of Microstrip Linear phased array antenna using integrated array feeder » King Fahd University of Petroleum & minerals, Dahran, Saudi Arabia, Dec 2005

[3] AJAL.A.J, «Antenna arrays» Department Of Ece Eniversal Engineering College, Vallivattom P.O, Thrissur, January 2014.

[4] C. A.Balanis, Antenna Theory Analysis And Design -3rd Edition, New Jersey: John Wiley & Sons, 2016.

[5] SANISH VS, Gana U Kamar, «Millimeter Wave Circular Microstrip Patch Antenna For 5 G Applications » Dept Of ECE, JCET JCE17ECCP03, S4 MTECH, India, 2019.

[6] Mohamed Amine Beldi, François Boone ,Dominic Deslandes « Design of Microstrip Power Dividers with Filtering Functions», Conference: Microwave Conference (EuMC), 42nd European, Canada,October 2012.

[7] Daniel D. Harty, «Novel Design Of A Wideband Ribcage-Dipole Array And Its Feeding Network», Worcester Polytechnic Institute, Department of Electrical and Computer Engineering, Massachusetts, USA, December 17th, 2010.

[8] Keith Benson «Phased Array Beamforming ICs Simplify Antenna Design » Analog Dialogue 53-01, California, USA, January 2019.

[9] Ratul Majumdar, Ankur Ghosh, Souvik Raha, Koushik Laha, and Swagatam Das «A Quantized Invasive Weed Optimization Based Antenna Array Synthesis with Digital Phase Control » Dept. of Electronics & Telecommunication Eng, Jadavpur University, Kolkata-700 032, India,2011.

[10] Juin Acharjee, Kaushik Mandal, Sujit Kumar Mandal, Partha Pratim Sarkar , « Mutual Coupling Reduction between Microstrip Patch Antennas by Using a String of H-Shaped DGS », International Conference on Microelectronics, Computing and Communications (MicroCom), Durgapur, India, January 2016.

[11] Hema Singh, H. L. Sneha, and R. M. Jha, « Mutual Coupling in Phased Arrays: A Review » Centre of Electromagnetics, CSIR-National Aerospace Laboratories, Bangalore 560 017, India, 2013.

[12] Iram Nadeem1, And Dong-You Choi « Study On Mutual Coupling Reduction Technique For MIMO Antennas » IEEE Access, Department Of Information And Communication Engineering, Communication And Wave Propagation Laboratory, Chosun University, Gwangju 61452 , South Korea, December 2018.

[13] K. Prahlada Rao1*, Vani R.M2, P.V. «Hunagund1four Element Microstrip Antenna Array With Electromagnetic Band Gap Structure And Silver Material Deposition For Reduced Mutual Coupling» Journal Of Science And Technology, Gulbarga University, Gulbarga, 585106, India, June 2019.

[14] P.V.N.Sumanth Reddy" Electromagnetic Band Gap In RF And Microwave Devices " Course In Slideshare, Department Of M.Sc Computer Science, S V University, Tirupat, India 2014.

[15] Fan YangY. Rahmat «Microstrip antennas integrated with electromagnetic band-gap (EBG) structures: a low mutual coupling design for array applications»IEEE Transactions on Antennas and Propagation, UCLA: University of California, Los Angeles,2003.

[16] Fadwa EL MOUKHTAFI[1] , Mohssin AOUTOUL[1] , Khalid SABRI[1] , Youssef ERRAMI[2] And Redouane JOUALI[3] « A Review On Mutual Coupling Reduction Methods For Antenna Arrays » Bdiot'19: Proceedings Of The 4th International Conference On Big Data And Internet Of Things, Article No.: 49University El-Jadida, Morocco , October 2019

[17] Ankit Pandey «Microstrip Patch Antenna With DGS », Research Scholar, Course NIT Delhi, May 2014.

[18] Poorna Pathak, Sunil Kumar Singh «A Survey Report On Isolation Techniques For Printed MIMO Antenna Systems » International Journal Of Engineering And Advanced Technology (IJEAT), ISSN: 2249 – 8958, Volume-7 Issue-2, India, December 2017.

[19] Shobit Agarwala «Newly Proposed Multi-Band Rectangular Patch Antenna Using Defected Ground Structures» Conference: Progress In Electromagnetic Research Symposium, At Nanyang Technological University, Singapore, November 2017.

[20] Shahrammohanna, Alifarahbakhsh, Saeedtavakoli,And Nasser Ghassemi, « Reduction Of Mutual Coupling And Return Loss In Microstrip Array Antennas Using Concave Rectangular Patches» , Hindawi Publishing Corporation International Journal Of Microwave Science And Technology Volume 2010, Article ID 297519, 5 Page. Faculty Of Electrical And Computer Engineering, The University Of Sistan And Baluchestan, Zahedan 9816745563, Iran, December,2010.

[21] Marwa Daaghari, Chafai Abdelhamis, Hedi Sakli, Kamel Nafakha «High Isolation With Neutralization Technique For 5G-MIMO Elliptical Multi-Antennas » Proceedings Of The 8th International Conference On Sciences Of Electronics, Technologies Of Information And Telecommunications (SETIT'18), Volume 2(Pp 124-133), Hammamet, Tunisia, 20–22 December 2018.

[22] Yohan Lim,[1] Young Joong Yoon, And Byungwoon Jung «Parasitic-Element-Loaded UWB Antenna With Band-Stop Function For Mobile Handset Wireless Usb» International Journal Of Antennas And Propagation, Volume 2012, Article Id 427841, Repubic of Korea, November 2012.

[23] Wai-Kai Chen, The Electrical Engineering Handbook **,** 2005.

[24] Raj Kumar[1], J. P. Shinde[2] And M. D. Uplane[3] «Effect Of Slots In Ground Plane And Patch On Microstrip Antenna Performance» International Journal Of Recent Trends In Engineering, Vol 2, No. 6, India, November 2009.

[25] Anuj Mehta, « Microstrip Antenna » International Journal Of Scientific & Technology Research Volume 4, Issue 03, Sydney, Australia, March 2015.

[26] A.Azrar, «Antennas "Microstrip Patch Antennas",» Institute Of Electrical And Electronic Engineering /University M'hamed Bougara, Boumerdes /Algeria.

[27] S. S. D. V. P. B. N. Sourabh Bisht, «Study The Various Feeding Techniques Of Microstrip Antenna Using Design And Simulation Using Cst Microwave Studio.,» International Journal Of Emerging Technology And Advanced Engineering Website: Www.Ijetae.Com(Issn 2250-2459, Iso 9001:2008 Certified Journal, Volume 4., India, September 2014).

[28] Houda Werfelli, Khaoula Tayari, Mondher Chaoui, Mongi Lahiani, Hamadi Ghariani «Design Of Rectangular Microstrip Patch Antenna », 2nd International

Conference On Advanced Technologies For Signal And Image Processing - ATSIP'2016, Monastir, Tunisia, National Engineers School Of Sfax Laboratory Of Electronics And Technology Of Information (LETI), Sfax, Tunisia, March 21-24, 2016

[29] Bablu Singh, «Microstrip patch-antenna», course, konkan gyanpeeth college of engineering, Mumbai, India, October 2015.

[30] Dr.T.Jayanthy, D.Rajeswari, Dr.S.Sathiyapriya, «Design And Simulation Microstrip Array Antenna Using Circular Patch In UWB Application», International Journal Of Advanced Research In Electronics And Communication Engineering (IJARECE) Volume 5, Issue 10, October 2016.

[31] Aissaoui Abderrahmane, REBAI Walid "Effect of Concavity and Slots Rectangular Patch Antennas " Institute of Electrical and Electronic Engineering, University of Boumerdes, Algeria. 2019

[32] Seevan F. Abdulkareem "Design and Fabrication of Printed Fractal Slot Antennas for Dual-band Communication Applications", Al-Mansour University College; irak, October 2013.

[33] Steve Jenson, Microstrip Patch Antenna, Northern Arizona University, December 14, 2010.

[34] P. A. Azrar, "Antennas "Fundamental Parameters Of Antennas"," Igee/Umbb, Boumerdes, Algeria.

[35] Prof. G.Kalpanadevi M.E, Ph.Dm.K.Nillopher Nishaw1 , E.Priyamalli2 , V.Radhika 3 , V.Shenbaga Priyanga4, "Design And Analysis Of Wilkinson Power Divider Using Microstrip Line And Coupled Line Techniques" Iosr Journal Of Electronics And Communication Engineering (Iosr-Jece) Pp. 34-40, E-Issn: 2278-2834, P-Issn: 2278-8735, Tamil Nadu, India, 2017.

[36] David. M. Pozar, "Microwave Engineering " 4th edition, John wiley and son's, 2011.

Appendix A:

CST MICROWAVE STUDIO

To refine the calculated results, we have used the COMPUTER SIMULATION TECHNLOGY MICROWAVE STUDIO (CST MWS) software instead of the IE3D software for [31]. CST is a 3D simulator that is based upon a Finite Integration Technique (FIT) very similar to the finite different time domain (FDTD) analysis one. Whereas IE3D is based on MoM solution which is not suitable for large antenna array application. Thus, for simpler shape like rectangular or circular, a slight difference in results may be obtained due to the difference in the methods of analysis and the algorithm of the EM simulation software, which is the case for us.

CST MWS is an efficient tool for 3D EM simulation enabling high accuracy simulation results for complex antenna structures and it specifically suitable for wideband antenna simulation. It has a much better interface which enables the user to include very fine details in the geometry of the simulated structure. This software offers a number of different solvers, mainly time and frequency domain for its high accuracy, and that's for a different types of application in a very high frequency range. The figure A.1 shows the different application the in CST software.

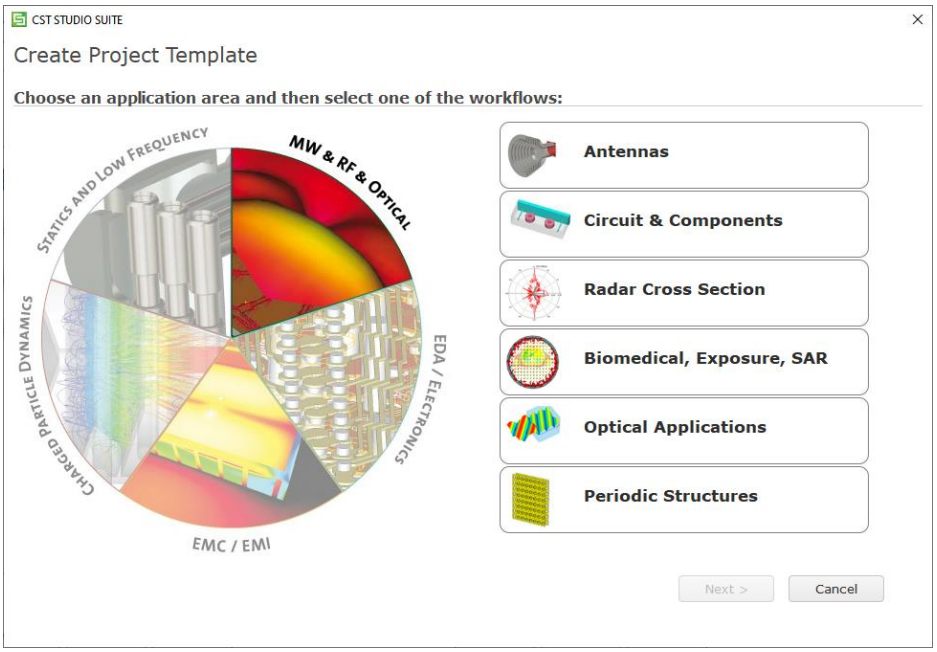

Figure A.1: Front page of CST showing the different application available.

CST is generally used in different type of antenna simulations, where all the parameters can be obtained like the S-parameters, input impedance, current distribution, VSWR, radiation patterns at all the planes as well as many other features that were very helpful during our simulations.